UNIVERSITY OF CALIFORNIA SAN DIEGO

The effects of RPL22 and RPL22L1 on early cell fate determination in an *in vitro* embryonic differentiation model

A Thesis submitted in partial satisfaction of the requirements
for the degree Master of Science

in

Bioengineering

by

Natalie Maloney

Committee in charge:

Professor Gene Yeo, Chair
Professor Stephanie Fraley, Co-Chair
Professor Adam Engler

2022

The Thesis of Natalie Maloney is approved, and it is acceptable in quality and Form for publication on microfilm and electronically.

University of California San Diego

2022

DEDICATION

To my wonderful family for supporting me through every endeavor and adventure. Thank you Halmoni and Halabogee for always showing me your unconditional love, mom and dad for your patience and guidance, and Alec for having my back no matter what.

TABLE OF CONTENTS

LIST OF ABBREVIATIONS

ABL22	APOBEC-RPL22 fusion construct
ABL22L1	APOBEC-RPL22L1 fusion construct
APOBEC1	Apolipoprotein B Editing Catalytic Subunit 1
BFP	Blue Fluorescent Protein
BMP4	Bone Morphogenetic Protein 4
BSA	Bovine serum albumin
Cas9	CRISPR-associated protein 9
CRISPR	Clustered Regularly Interspaced Short Palindromic Repeats
CVB	Coxsackievirus B3
CXCR4	C-X-C chemokine receptor type 4
DHFR	Dihydrofolate reductase
DMEM	Dulbecco's Modified Eagle's Medium
EB	Embryoid body
ECL	Enhanced chemiluminescence
FABP7	Fatty acid binding protein 7
FACS	Fluorescence-activated Cell Sorting
FBS	Fetal bovine serum
GAPDH	Glyceraldehyde-3-phosphate dehydrogenase
GFP	Green Fluorescent Protein
HRP	Horseradish peroxidase
KDR	Kinase insert domain receptor
KLF4	Krüppel LIke Factor 4

KRAB	Krüppel Associated Box
NeuroD1	Neurogenic differentiation 1
Oct4	Octamer-binding transcription factor 4
PAM	Protospacer Adjacent Motif
PBS	Phosphate-buffered saline
PCR	Polymerase Chain Reaction
PDGFRA	Platelet-derived growth factor receptor A
qPCR	Quantitative PCR
RPL22	Ribosomal Protein 22
RPL22L1	Ribosomal Protein 22-Like
RIPA	Radioimmunoprecipitation assay buffer
ROCK	Rho-associated protein kinase
RT-PCR	Reverse transcription polymerase chain reaction
SDS	Sodium dodecyl sulfate
SDS-PAGE	Sodium dodecyl sulfate polyacrylamide gel electrophoresis
SMAD	Suppressor of Mothers against Decapentaplegic
STAMP	Surveying Targets by APOBEC Mediated Profiling
TBST	Tris-buffered saline with 0.1% Tween® 20 detergent
TGT-β	Transforming growth factor - β
TMP	Thymidine monophosphate

LIST OF FIGURES

LIST OF TABLES

ACKNOWLEDGEMENTS

I want to express my deepest appreciation to my mentor Elliot Chen for his never ending guidance throughout my research experience. Everything I have learned I can attribute to him and his teachings. Elliot was patient, thorough, and always willing to go out of his way to help me. I cannot thank him enough for all he has done for me.

I would also like to acknowledge Professor Gene Yeo, an amazing principal investigator and chair of my thesis committee. From the start, he was so welcoming, engaging, and as eager as I was to get me started in his lab. It was also due to his wonderful idea that I was matched with Elliot as my mentor.

ABSTRACT OF THE THESIS

The effects of RPL22 and RPL22L1 on early cell fate determination in an *in vitro* embryonic differentiation model

by

Natalie Maloney

Master of Science in Bioengineering

University of California San Diego, 2022

Professor Gene Yeo, Chair
Professor Stephanie Fraley, Co-Chair

Due to the discovery of ribosome heterogeneity, there has opened a huge field of research surrounding the regulatory roles that ribosomal proteins play in cellular functions. Understanding how each one affects cell growth, differentiation, and maturation will build a more robust model of cellular development. This study aimed to analyze the effects of RPL22 and its paralog,

RPL22L1, on early cell fate determination in an *in vitro* embryonic differentiation model. To do this, we generated RPL22 and RPL22L1 knockdown lines using the CRISPRi platform in iPSCs. These cell lines were then used for embryoid body (EB) formation in order to study the effects of RPL22 and RPL22L1 in the development of the three germ layers by accessing the expression of cell lineage markers during differentiation. We found that RPL22L1 can compensate for the loss of RPL22, but the opposite is not true, and that RPL22L1 is essential for cell survival and EB differentiation. Our results also suggest that RPL22 may contribute to definitive endoderm development, affect differentiation of mesoderm-derived cell types, and play a positive role in neuron differentiation. Finally, we adapted a new technology, Surveying Targets by APOBEC Mediated Profiling (STAMP), and successfully synthesized APOBEC-RPL22 and APOBEC-RPL22L1 constructs so that we can identify the translational and RNA binding targets of RPL22 and RPL22L1 to gain insight into the molecular mechanisms they may regulate.

INTRODUCTION

Ribosome heterogeneity

Ribosomes were traditionally thought to be passive translational ribonucleoprotein complexes with no regulatory functions. It was once believed that all ribosomes were uniform in both composition and structure across all cell types. It was not until the 1980s and 1990s that variation amongst ribosomes was discovered and more closely studied, thereby determining ribosome heterogeneity[1]. Ribosomes can differ across cell types or even subcellular regions within a single cell. Mature ribosomes have been found to change their composition or structure in response to different stimuli, implying that ribosome heterogeneity is dynamic[1]. Ribosomes have been found to be heterogeneous in a variety of ways, and the source of their heterogeneity can be attributed to multiple sources. They can undergo varying cytoplasmic changes such as post-translational or rRNA modifications, or attachment of ribosome-associated proteins. In the nucleus during ribosome biogenesis, ribosomes may be synthesized from rRNA variants and different ribosomal proteins, or may only differ by paralogues[1]. Ribosomal protein paralogs are highly homologous to each other, but can alter the translational and regulatory properties of a ribosome. An example would be Ribosomal Protein 22 (RPL22) and its paralog Ribosomal Protein 22-Like (RPL22L1), which are the focus of this study.

In terms of the functions of the ribosome, ribosome heterogeneity allows them to play a regulatory role in gene expression. Different compositions of ribosomal proteins may be specialized to translate small subsets of mRNAs, or be more efficient at translating those mRNAs. For example, in a previous study it was found that ribosomes containing RPS25 or RPL10a/L1, but not RPL22, preferentially translated a specific set of several hundred mRNAs that are all functionally related[2]. This means that these specialized ribosomes can control cellular

functions based on their translation efficiency for certain genes. Determining which ribosomal proteins regulate which genes can help us gain insight into cellular processes such as metabolism, the cell cycle, embryonic development, and disease development.

Ribosomal Protein Paralogs RPL22 and RPL22L1

In a preliminary screening conducted in the lab, we sought to identify ribosomal protein candidates in cell fate determination for further investigation. In the screening, each ribosomal protein was knocked down in iPSC-derived embryoid bodies and its effects were analyzed via single cell sequencing. From the preliminary results, RPL22 was discerned as a candidate having a significant effect on certain subsets of cells. Knockdown of RPL22 created a strong variation in the enrichment of differentiated cell types when compared to the non-targeting cells. Given the substantial effects seen due to RPL22 knockdown, we decided to focus our research on RPL22 and its paralog, RPL22L1, to study which genes they regulate and how it might affect cell fate.

Ribosomal protein paralogs are nearly identical in sequence, yet inflict exceptionally different effects on cellular processes, of which RPL22 and RPL22L1 are no exception (Figure 1). In a study conducted in zebrafish, Zhang et al. discovered that knockdown of RPL22 blocked the development of T-cell progenitors while knockdown of RPL22L1 inhibited differentiation into hematopoietic stem cells due to their antagonistic effects on SMAD1 expression[3]. In another study, it was found that RPL22 induces exon 9 skipping of SMAD2 pre-mRNA while RPL22L1 has the opposite effect and induces exon 9 inclusion[4]. Together, RPL22 and RPL22L1 regulate Nodal/TGT-β signaling which is important in many cellular processes such as cell proliferation, differentiation, and migration[5]. These two studies demonstrate that RPL22 and its paralog, RPL22L1, have vastly different effects on cellular processes but both are required for those

processes to function properly. It is crucial to study the differences in translational control between ribosomal protein paralogs in order to better understand how they are involved in the regulation of cellular functions.

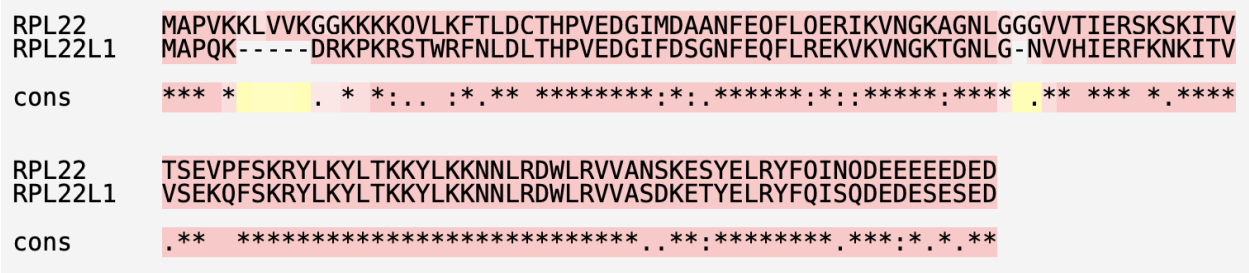

Figure 1: Alignment of RPL22 and RPL22L1 protein sequences. Much of their sequences are conserved between each other, indicating that they are highly homologous.

CRISPR-interference (CRISPRi)

In order to study which genes may be affected by RPL22 and RPL22L1 and how they regulate those genes, we employed a CRISPR-interference (CRISPRi) system to knockdown both ribosomal proteins. CRISPRi is derived from the CRISPR/Cas9 genome editing platform. In brief, this system uses a CRISPR-associated protein 9 (Cas9) that is guided by a single guide RNA (sgRNA) to its encoded DNA target sequence. Cas9 has endonuclease activity which allows it to create a double-strand break in the target region of the DNA when it binds to its protospacer adjacent motif (PAM), a short DNA motif on the 3' end of the DNA target sequence[6]. This mechanism silences the expression of the gene of interest via genome editing, allowing its user to study the effects of its knockout.

CRISPR knockout results in complete loss of function of the target gene. For genes that are essential, as most ribosomal proteins are, knocking them out is lethal and will result in cell death, preventing us from studying their effects. CRISPRi is an attractive alternative to this method because it allows for transcription regulation, or knockdown, rather than complete

knockout. In the CRISPRi system that is used in this study, Cas9 is catalytically inactivated such that it no longer has endonuclease activity (dCas9). In order to efficiently knockdown the target gene, dCas9 is fused to a Krüppel-associated box (KRAB) transcriptional repression domain. When the dCas9-KRAB fusion protein is guided by gene specific sgRNA to the promoter region of the DNA target sequence, the KRAB transcription repression domain then represses the target gene transcription[7] (Figure 2). This mechanism prevents cell death that might occur when knocking out an essential protein, allowing for the further investigation of how knockdown of the gene of interest impacts cell processes.

In addition to its gene inactivation abilities, our CRISPRi platform is inducible, reversible, and highly specific[8]. It has also been found that the CRISPRi system can simultaneously control the expression of multiple genes[9]. This feature can be useful when trying to study the combined effect of genes belonging to the same functional group. Taken in total, the CRISPRi system is highly customizable, making it an attractive tool to use when studying the regulatory effects of specific proteins, in our case, RPL22 and RPL22L1.

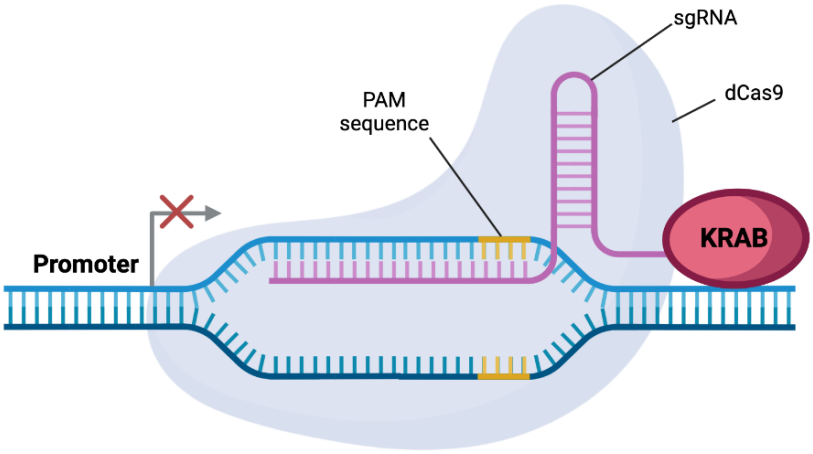

Figure 2: Diagram of CRISPRi mechanism. dCas9-KRAB complex is guided by an sgRNA to its encoded DNA target sequence in the promoter region of the target gene. dCas9 binds to its PAM sequence and the KRAB transcription repression domain then represses the target gene transcription, preventing expression of the target gene.

Given that previous studies have validated ribosome heterogeneity and found regulatory differences between RPL22 and RPL22L1 in various models, we decided to explore their differences during early embryonic development. Using CRISPRi technology, we aimed to knockdown the expression of RPL22 and RPL22L1 in iPSCs in order to study their regulatory effects in cell proliferation and differentiation. To do so, we analyzed the expression of various cell lineage markers as a result of knockdown in a differentiated model using embryoid bodies (EBs), cell aggregates containing the structure of early embryos and cells of all three germ layers. This research will give us insight into the role that RPL22 and RPL22L1 play in early human embryonic development and cell fate determination.

Surveying Targets by APOBEC Mediated Profiling (STAMP)

In addition to understanding how RPL22 and RPL22L1 influence early differentiation and cell fate, we wanted to go one step further and investigate the mechanism behind their regulation by identifying their translational or RNA binding targets. To do this we employed a new technology called STAMP (Surveying Targets by APOBEC Mediated Profiling), which utilizes Apolipoprotein B Editing Catalytic Subunit 1 (APOBEC1) and RNA sequencing (RNAseq)[10]. APOBEC1 is a cytidine to uridine single-stranded RNA (ssRNA) editing enzyme that, when fused to a RNA binding protein (RBP), has the ability to edit a target sequence proximal to its binding sites[10,11]. Using RNAseq to find the regions with cytidine to uridine conversions, we can then identify the RNA binding sites of APOBEC1 fused RNA binding proteins of interest. By designing an APOBEC fusion protein with RPL22 and RPL22L1, we can gain insight into whether they affect the translation of different subsets of genes or have different RNA targets.

In this study, we developed a CRISPRi iPSC cell line to knockdown RPL22 and its paralog, RPL22L1. We then performed assays to confirm knockdown at the protein and RNA level for both ribosomal proteins. Following validation, we analyzed the expression of pluripotency genes as a result of knockdown to determine whether RPL22 and RPL22L1 impacted maintenance of iPSCs in the pluripotency state. To study the effects of RPL22 and RPL22L1 knockdown in early embryonic development, we used EBs as our differentiation model to determine whether our ribosomal proteins of interest altered the RNA levels of other ribosomal proteins and cell lineage markers. Additionally, we generated APOBEC fusion proteins with RPL22 and RPL22L1 to identify their exact translational or RNA binding targets. Data gathered from these experiments will help us understand the regulatory roles of RPL22 and RPL22L1 in cell fate determination, and how those roles differ from each other.

METHODS

Generating CRISPRi iPSC Cell Line

To knockdown the ribosomal proteins of interest, a stable CRISPR-interference (CRISPRi) iPSC line was generated following the protocol published by Tian et al[8]. To summarize, the expression cassette of DHFR-dCas9-BFP-KRAB in the plasmid pRT029 (Addgene #127969) was inserted into the CLYBL safe harbor locus of Coxsackievirus B3 (CVB) induced pluripotent stem cells (iPSCs) (Coriell GM25430) by co-transfection with spCas9 nuclease protein (Synthego) and a CLYBL locus-targeting sgRNA (Synthego, sequence ATGTTGGAAGGATGAGGAAA). The diagram in Figure 3 illustrates this synthesis. This enables a robust transgene expression and minimizes the risk of perturbing local gene expression. After co-transfection and cell expansion, the BFP-positive cells were isolated via Fluorescence-activated Cell Sorting (FACS) sorting, and a stable single cell clone with robust expression of dCas9-BFP-KRAB was isolated from the selected pool via single colony selection and used for target gene perturbation experiments.

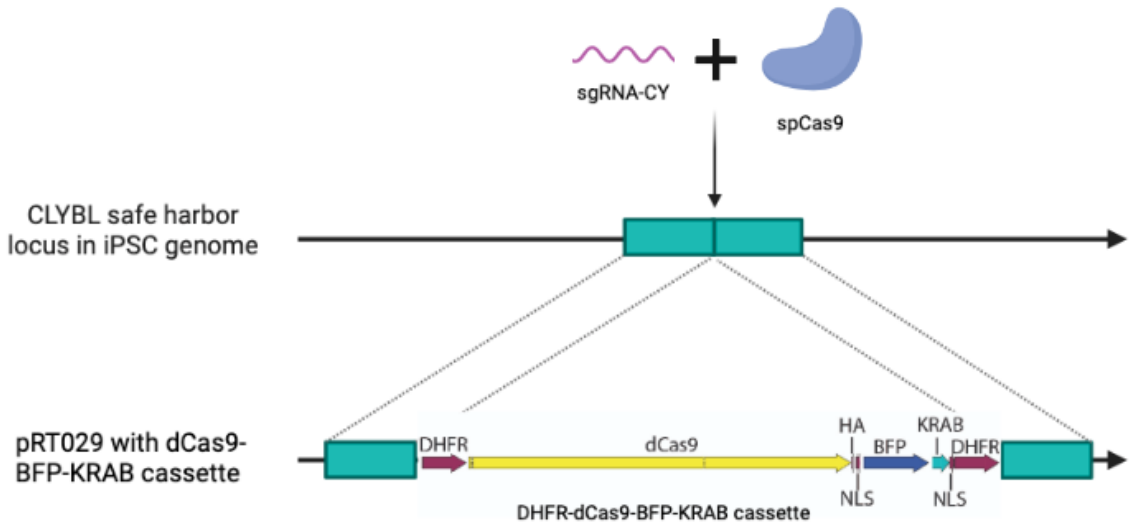

Figure 3: Diagram depicting the generation of the CVB iPSC genome containing the dCas9-BFP-KRAB cassette. The expression cassette of DHFR-dCas9-BFP-KRAB was inserted into the CLYBL safe harbor locus of CVB iPSCs by co-transfection with spCas9 nuclease protein and a CLYBL locus-targeting sgRNA.

Cloning

sgRNA Cloning

For sgRNA cloning, all sgRNA plasmids were assembled using the pMK1334 lentiviral vector. The pMK1334 plasmid was digested by BlpI and BxtXI with 10X FastDigest Green buffer (Thermo Fisher Scientific). The digested vector was then run on 0.8% agarose gel in order to separate the digested vector from the uncut vector and other undesired fragments. The gel was stained by SYBR Safe DNA Gel Stain (Invitrogen), and the linearized vector was cut from the gel and purified using the Qiagen QIAquick Gel Extraction Kit according to the manufacturer's protocol. The RPL22 and RPL22L1 sgRNA sequences were designed based on the Human Genome-wide CRISPRi-v2 Libraries (Addgene #83969) and the Human CRISPR Inhibition Pooled Library (Dolcetto, Addgene #92385). All sgRNA sequences can be found in Table 1. All sgRNAs were ordered from Integrated DNA Technologies (IDT) as two oligos according to the following format:

Top oligo: TTG-sgRNA-GTTTAAGAGC

Bottom oligo: CTTGTTG-sgRNA-GTTAAGAGCTAA

The reverse complement of the bottom oligo was used for annealing to the top oligo. The annealed oligos were used for direct ligation with the digested pMK1334 vector by T4 DNA ligase (New England Biolabs). The diagram in Figure 4 illustrates this workflow.

Table 1: List of sgRNAs used to knockdown RPL22 and RPL22L1 and their corresponding sequences.

sgRNA Name	Sequence
sgRPL22-1	CCTGGAGCCGAGGCCTCACG
sgRPL22-2	GCTAACCACAGGAGCCATGG
sgRPL22L1-1	GGAGTGAGCGATGTCTTGGT
sgRPL22L1-2	GTCGCGGCCGACTCGCAAGA

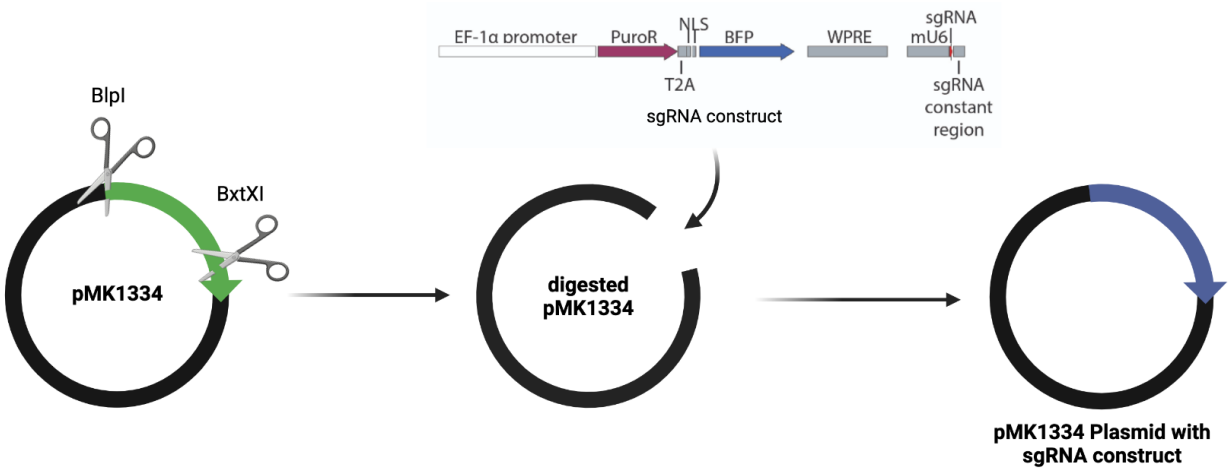

Figure 4: Diagram depicting the workflow to synthesize the pMK1334 plasmid containing the sgRNA construct for RPL22 and RPL22L1. The pMK1334 plasmid was first digested with BlpI and BxtXI restriction enzymes, and then the sgRNA construct was ligated with the digested vector.

The fully assembled products were transformed via heat shock using a 42℃ water bath into NEB 5-alpha competent cells (New England Biolabs) and plated on agar plates with Ampicillin. The plates were incubated at 37ºC and the bacteria were allowed to grow overnight before picking colonies. The picked colonies were then cultured in LB medium for 16 hours at 37ºC. Lastly, the ZymoPURE™ Plasmid Midiprep Kit was used for plasmid purification of the bacteria according to the manufacturer's protocol. To validate the sequences, two clones of each sgRNA plasmid were sent to the Genewiz (Azenta Life Sciences) for sequencing.

pLVX Cloning

To express the APOBEC1-RPL22 and -RPL22L1 fusion proteins in the cells, gBlock gene fragments of APOBEC1-RPL22-3×Flag and APOBEC1-RPL22L1-3×Flag were ordered from IDT which contained EcoRI and AgeI restriction sites on the 5' and 3' ends, respectively. The gBlocks were digested with EcoRI and AgeI, and cleaned up with the Zymo DNA clean & concentrator kit (Zymo Research) according to the manufacturer's protocol. The digested

gBlocks were then ligated with the pLVX-TetOne-Puro-hAXL plasmid (Addgene #124797), which was also EcoRI and AgeI digested and gel purified, to generate the pLVX-TetOne-APOBEC1-RPL22-3×Flag-Puro (pLVX-ABL22) and pLVX-TetOne-APOBEC1-RPL22L1-3×Flag-Puro (pLVX-ABL22L1) plasmids (Figure 5).

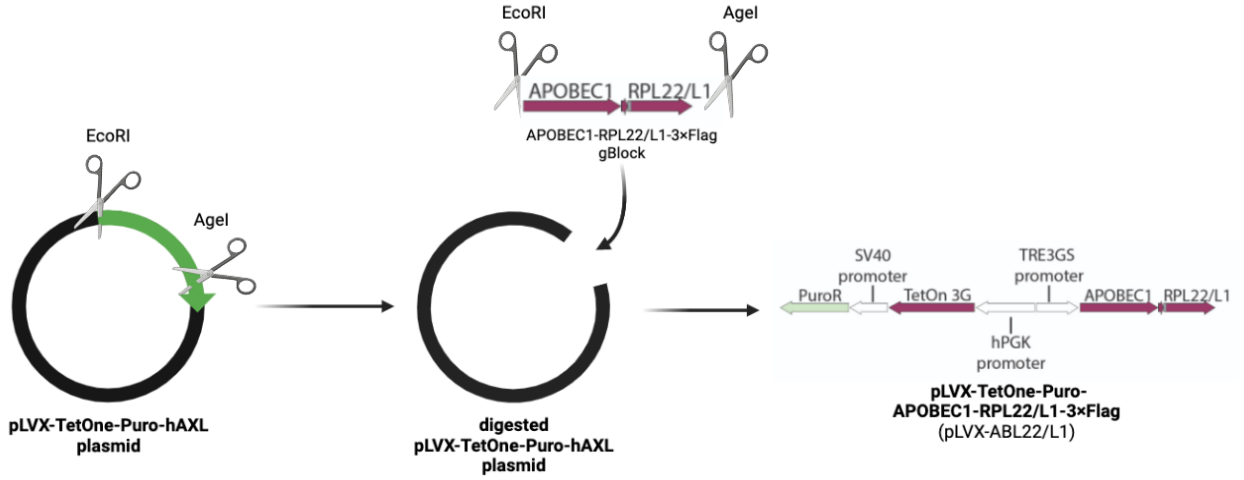

Figure 5: Diagram depicting the workflow to synthesize the plasmid containing the pLVX-TetOne-APOBEC-RPL22/L1-3xFlag-Puro cassette. The pLVX-TetOne-Puro-hAXL plasmid and APOBEC-RPL22/L1-3xFlag gBlocks were both digested with EcoRI and AgeI restriction enzymes, and then ligated together.

After confirming the sequences via sequencing, the plasmid was used to generate a similar construct where the Puromycin-resistant gene was replaced with TurboGFP. To make the constructs, two fragments were PCR amplified. The first fragment was generated by PCR amplification of the TetOn3G sequence from the pLVX-ABL22 or pLVX-ABL22L1 plasmids using the following primers:

Forward primer: GGGATCATCGAATTACCATGTCTAG

Reverse primer: CGCGTTTTGCAAAAGCCTAGGC

The second fragment was generated by PCR amplification of GFP sequence from the pCW57-GFP-2A-MCS plasmid (Addgene #71783) using the following primers:

Forward primer: CTAGGCTTTTGCAAAACGCGACCATTCGCCACCATGGAGAGCGAC

Reverse primer: TCCAGAGGTTGATTGTTCCAGACUATTCTTCACCGGCATCTGCATCC

All PCR reactions were performed using NEBNext® Ultra™ II Q5® Master Mix ((New England Biolabs), amplified for 25 cycles, and purified with the Zymo DNA clean & concentrator kit. Two PCR amplified fragments were inserted into the XbaI and MluI digested pLVX-ABL22 and pLVX-ABL22L1 plasmids by NEBuilder® HiFi DNA Assembly (New England Biolabs) to generate the pLVX-ABL22-GFP and pLVX-ABL22L1-GFP.

All fully assembled products were transformed via heat shock using a 42℃ water bath into NEB 5-alpha competent cells and plated on agar plates with Ampicillin. The plates were incubated at 37°C and the bacteria were allowed to grow overnight before picking colonies. The picked colonies were then cultured in LB medium for 16 hours at 37°C. Lastly, the ZymoPURE™ Plasmid Midiprep Kit was used for plasmid purification of the bacteria according to the manufacturer's protocol. To validate the sequences, all isolated plasmids were sent to Primordium for full plasmid sequencing.

Lentivirus Production for sgRNA and pLVX Clones

All lentivirus production was done in 293T cells that were cultured in Dulbecco's Modified Eagle's Medium (DMEM) with 10% FBS and PenStrep in an incubator at 37^0C. For each transfection, 1×10^6 293T cells were plated in a well of 6-well plate a day before transfection. The next day, 1.92 μg of each validated sgRNA or pLVX clone was co-transfected with 1.6 μg packaging vector psPAX2 and 0.64 μg envelope vector pMD2G into the plated 293T cells using the Lipofectamine™ 3000 Reagent (Invitrogen). The transfected 293T cells were cultured in DMEM with 10% FBS in an incubator at 37^0C overnight. The day following

transfection, the medium was changed. Two days after medium change, the lentivirus for each sgRNA and pLVX clone was harvested and filtered through a 0.45 μm filter into a collection tube. The lentiviral stocks were then concentrated 40-fold following the Lenti-X™ Concentrator Protocol (Clonetech) and stored at -80℃.

Cell Culture and sgRNA Lentivirus Transduction

CVB-iPSC and its derived CRISPRi cell lines were cultured on Matrigel coated plates (Corning) with mTesR Plus medium (STEMCELL Technologies) and split with Gentle Cell Dissociation Reagent (STEMCELL Technologies) once reaching about 80% confluency. For lentivirus transduction, the cells were counted using a Bio-Rad TC10™ Automated Cell Counter and 1 x 10^5 cells were plated per well (9.5 cm^2 surface area) with the treatment of 10 μM ROCK inhibitor (Y-27632, TOCRIS). Once plated, 15 μL of lentivirus stock was immediately added to each well. For the transduction with the pLVX-ABL22-GFP and pLVX-ABL22L1-GFP lentivirus stocks, the cells were expanded and will be FACS sorted to select a pure cell population with pLVX-ABL22-GFP and pLVX-ABL22L1-GFP expression. To induce the knockdown of the target genes in sgRNA lentivirus infected cells, 20 μM of trimethoprim (TMP) was treated for two days. After TMP treatment, the cells were harvested for protein and RNA isolation to examine the efficiency and the effects of the knockdown.

Total Protein Isolation

Once the cells reached 80-90% confluency, two to four wells of a 6-well plate of each cell line were washed with phosphate-buffered saline (PBS) and then 200 μL lysis buffer (1X RIPA Buffer (Millipore Sigma), 1% sodium dodecyl sulfate (SDS), and protease inhibitor

cocktail set III (Millipore Sigma)) was added to each well. The lysed cells of each cell line were subsequently scraped down and combined into a collection tube, and sonicated for at least 10 cycles on a Bioruptor Plus Sonication device (Diagenode Diagnostics, 30 second on and 30 second off per cycle) at 4℃. After sonication, protein lysates were centrifuged at 16,000 g for 10 min at 4℃, and the supernatants were saved and used for further analysis.

Protein Assay

The concentration of all the protein samples was determined by using the *DC* protein assay (Bio-rad) per the manufacturer's protocol. Bovine serum albumin (BSA) dilutions of 2, 1.5, 1, 0.75, 0.25, 0.15, and 0 mg/mL were used as the standard and 1/5 and 1/7 dilutions were made for each protein sample. Both the standard and protein samples were loaded in triplicates so that an average could be used to calculate the concentration. All outliers were removed before calculations. The absorbance of each sample was measured using the Infinite 200 Pro (Tecan Life Sciences) plate reader at a wavelength of 750 nm. All absorbance readings were averaged and then that of the BSA standards were used to do a linear regression in Excel with the concentration on the y-axis and average absorbance on the x-axis. The slope (m) and y-intercept (b) of the line ($y = mx + b$) generated was used to calculate the uncorrected concentration (y) of each protein sample using the average absorbance reading (x). The corrected concentration was calculated by dividing the uncorrected concentration by its dilution, i.e. $\frac{calculated\ concentration\ (mg/ml)}{dilution\ (1/5\ or\ 1/7)}$, and then averaging this value with that of the other dilution.

SDS-PAGE analysis and Western blot

35 µg of each protein sample was loaded onto NuPAGE™ 4-12% Bis-Tris Gels (Thermo Fisher Scientific) and run at 150V for about 80 min in 1x NuPAGE™ MOPS SDS Running Buffer (Thermo Fisher Scientific). The protein samples were then wet-transferred from the gel to a Amersham™ Protran® Western blotting nitrocellulose membrane (Millipore Sigma) at 200 mA for two hours at 4℃. After the transfer was completed, the membrane was blocked with a 5% milk solution for 1 hour on a rocker.

Following membrane blocking, the membrane was probed with a primary antibody in a 5% milk mixture overnight at 4°C on a rocker. The primary antibodies that were used in this study and the respective dilution ratios are as follows:

RPL22: SC-136413, 1:1000, α-mouse (Santa Cruz)

RPL22L1: HPA048060, 1:1000, α-rabbit (Millipore Sigma)

GAPDH: ab8245, 1:2000, α-mouse (Abcam)

The next day, the membrane was washed 3 times for 5 min each with Tris-buffered saline with 0.1% Tween® 20 detergent (TBST), and then incubated with the appropriate HRP-conjugated secondary antibody (1:2500) in a 5% milk mixture for 40 min at room temperature on a rocker. After secondary incubation, the membrane was washed 3 times for 5 min each before developing. To develop the membrane, the membrane was incubated with the Pierce™ ECL Plus Western Blotting Substrate (Thermo Fisher Scientific) for 5 min, and the target protein images were captured by the Azure c600 Gel Imaging System (Azure Biosystems). In order to quantify and normalize the target protein level, the membrane was stripped using ReBlot Plus Strong Antibody Stripping Solution (Millipore Sigma) according to the manufacturer's protocol, and subsequently probed with GAPDH primary antibody following the same protocol.

EB Formation

To prepare embryoid bodies (EBs) for all CVB-iPSC CRISPRi lines, 24-well AggreWell™ 800 Microwell Plates (StemCell Technologies) were used. The wells of the AggreWell plates were pre-treated with Anti-Adherence Rinsing Solution (StemCell Technologies) and washed one time with mTeSR™ Plus medium. All cells were dissociated with Accutase™ Cell Dissociation Reagent (Thermo Fisher Scientific) and resuspended with mTeSR™ Plus Medium (StemCell Technologies) with ROCK Inhibitor (10 μM). The resuspended cells were then filtered through a 40μm strainer to dissociate into single cells. The cells were then counted and resuspended in mTeSR Plus medium with ROCK Inhibitor (10 μM). 3 x 10^6 cells were seeded per well and were then spun at 100 *xg* for 3 min. After spin down, the cells were incubated overnight at 37ºC.

The next day, the EBs were resuspended from the AggreWell plates and size selected using a 37 μm Reversible Strainer (StemCell Technologies) to filter out the single cells and small EBs such that only EBs larger than the mesh size were collected. All EBs were rinsed and collected in AggreWell™ Embryoid Body (EB) Formation Medium (Stemcell Technologies), and then transferred into Corning® Costar® Ultra-Low Attachment 6 Well Plates. EBs from each well in the 24-well microplate were aliquoted into two wells of the 6-well low attachment plate, for a total of eight wells per sgRNA. Four of the eight wells were treated with TMP. The transferred EBs were incubated overnight at 37ºC on a shaker to prevent them from fusing together. The following day, each well was split into two wells of about equal number of EBs to allow them more room to grow and help increase uniformity. Medium was changed daily for 5 days, after which the medium was changed every 2-3 days, and the EBs were continuingly cultured on a shaker till the end of the experiment. The EBs treated with TMP continued to be

treated with TMP throughout the whole experiment. On day 7, 14, and 21 of EB formation, two wells of each EBs were harvested for RNA isolation. The harvested EBs were washed with PBS and stored in 200 µL of DNA/RNA Shield (Zymo Research) at -20ºC until all time points were harvested.

RNA Extraction, Reverse Transcription, and Quantitative PCR

The cells that were destined for RNA analysis were washed with phosphate-buffered saline (PBS) and then 200µL DNA/RNA Shield (Zymo Research) was added to each sample. RNA extraction for all samples was carried out using the Quick-RNA™ MiniPrep Plus kit (Zymo Research) according to the manufacturer's protocol. The purified RNA samples were then used for reverse transcription polymerase chain reaction (RT-PCR) using the SuperScript™ IV First-Strand Synthesis System (Thermo Fisher Scientific) according to the manufacturer's protocol. The newly synthesized cDNA was employed in quantitative PCR (qPCR) using Power SYBR™ Green PCR Master Mix (Applied Biosystems) in the CFX Opus 384 Real-Time PCR System (Bio-Rad). Table 2 contains the list of pluripotency and differentiation markers that were used for qPCR. All primers were ordered from IDT. Duplicates for each differentiation marker were measured to increase accuracy. The output Ct values were subsequently used for data analysis.

Table 2: List of pluripotency genes, ribosomal proteins, housekeeping genes, cell lineage markers used in qPCR to analyze effects of RPL22 and RPL22L1 knockdown.

Pluripotency Markers	Mesoderm Markers	Ectoderm Markers	Endoderm Markers	Ribosomal Proteins	Housekeeping Genes
Pou5F1 (Oct4) NANOG KLF4 c-Myc	T PDGFRA KDR BMP4 p53	SOX1 Nestin FABP7 STMN2 NeuroD1	GATA4 GATA6 WNT3 CXCR4	RPL22 RPL22L1 RPL36AL RPL10A	GAPDH

Data Analysis

The Ct values were used to calculate the relative fold change in gene expression for each sample's pluripotency and differentiation markers (DM) across all time points using the delta-delta Ct ($2^{-\Delta\Delta Ct}$) method. All calculations were done on Excel. First, the change in Ct (ΔCt_{sample}) was found by averaging the two technical replicate Ct values of GAPDH (Ct_{GAPDH}) for NTC (-TMP) day 0, and subtracting it from the Ct value of the sample (Ct_{sample}). Next, delta-delta Ct ($\Delta\Delta Ct_{sample}$) was found by the following equation:

$$\Delta\Delta Ct_{sample} = \Delta Ct_{sample} - \Delta Ct_{cal}$$

where

$$\Delta Ct_{cal} = \left(\left(\frac{Ct_{DM-NTC(-TMP)\ Day\ 0,\ rep\ 1} + Ct_{DM-NTC\ (-TMP)\ Day\ 0,\ rep\ 2}}{2}\right) - \left(\frac{Ct_{GAPDH-NTC\ (-TMP)\ Day\ 0,\ rep\ 1} + Ct_{GAPDH-NTC(-TMP)\ Day\ 0,\ rep\ 2}}{2}\right)\right.$$

Then $2^{-\Delta\Delta Ct}$ was calculated for each sample, which was used to calculate the fold change of each sample using the following equation:

$$fold\ change = 2^{-\Delta\Delta Ct} \div \left(\frac{2^{-\Delta\Delta Ct}_{NTC\ (+TMP)\ Day\ 0,\ rep1} + 2^{-\Delta\Delta Ct}_{NTC\ (+TMP)\ Day\ 0,\ rep2}}{2}\right)$$

Finally, the fold change between both replicates was averaged and a standard deviation (SD) was calculated. The average fold changes and SDs were graphed on Prism 9 to visualize the results.

RESULTS

Downregulation of RPL22 and RPL22L1 in iPSCs via CRISPR interference

To study the roles of RPL22 and RPL22L1 in early cell-fate determination, the CRISPR interference (CRISPRi) system was used to knockdown the expression of RPL22 and RPL22L1 in iPSCs. The degron-based inducible CRISPRi platform for genetic knockdown of target genes in iPSCs that was used in this study was generated in the lab by adapting a published protocol[8]. sgRNAs targeting either RPL22 or RPL22L1 and a non-targeting control (NTC) sgRNA were cloned in the pMK1334 vector and prepared as lentivirus to transduce the iPSC CRISPRi cells. To validate the knockdown efficiency of RPL22 and RPL22L1 in the corresponding sgRNA lentivirus transduced cells, a western blot was performed (Figure 6). For the cells with RPL22 sgRNAs, sgRPL22-1 and sgRPL22-2, a significant reduction of RPL22 protein level was observed for both sgRNAs upon TMP treatment when compared to the samples with no TMP, as well as compared to that in the NTC. In addition, we also observed that knockdown of RPL22 resulted in increased expression of RPL22L1 protein levels. As shown in Figure 6C, RPL22L1 protein levels increased about 6-fold upon RPL22 knockdown by both RPL22 sgRNAs with TMP treatment when compared to that in the NTC sgRNA. It appears as though when RPL22 is downregulated, the cells compensate by significantly upregulating RPL22L1, and the result is consistent with previous studies[12]. Additionally, a potential leaky knockdown of RPL22 protein and induction of RPL22L1 protein by sgRPL22-2 was observed even without TMP treatment when compared to that in the NTC sgRNA. In contrast, this was not the case for sgRPL22-1, suggesting that sgRPL22-1 is a more effective sgRNA.

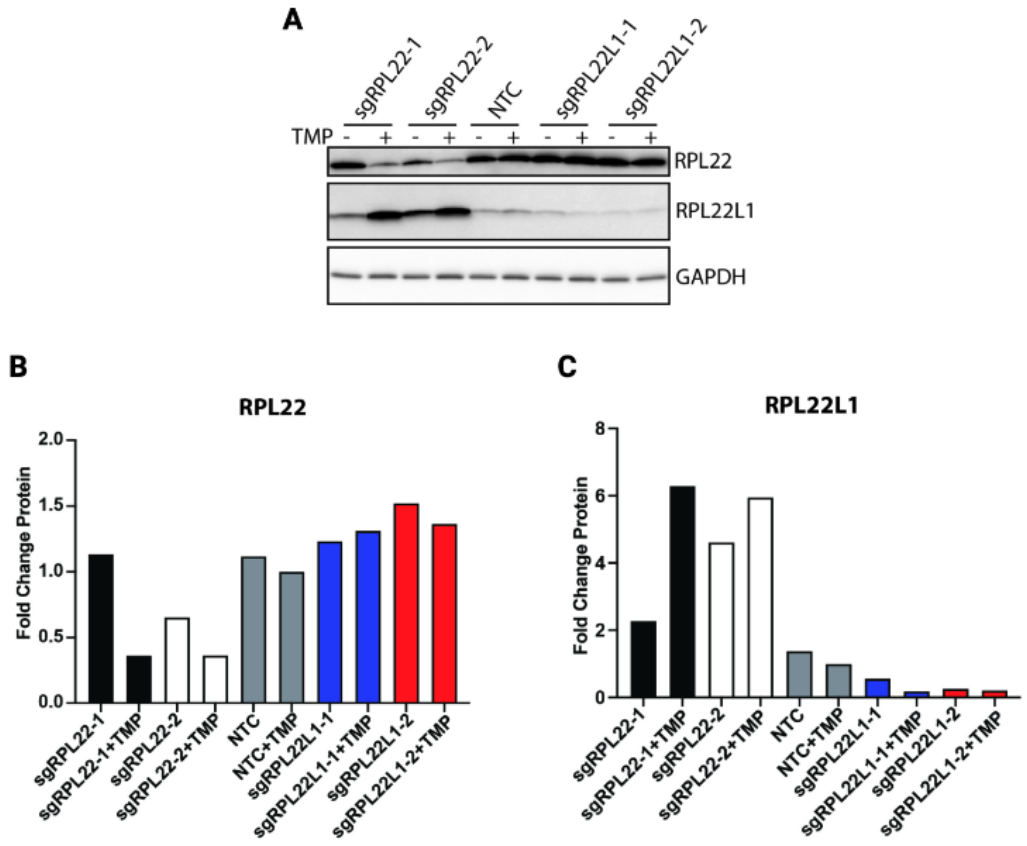

Figure 6: Western blot analysis of RPL22 and RPL22L1 knockdown. (A) Western blot images of various cell lines (+/-TMP) probed with RPL22, RPL22L1, and GAPDH. The protein levels of RPL22 and RPL22L1 were normalized to GAPDH. Fold changes of RPL22 and RPL22L1 were calculated relative to the amount in NTC. (B) Graph of the RPL22 protein fold change in various cell lines (+/-TMP). There is knockdown of RPL22 in the induced sgRPL22 cell lines (black and white) compared to the NTC (gray). (C) Graph of the RPL22L1 protein fold change in various cell lines (+/-TMP). There is knockdown of RPL22L1 in the induced sgRPL22L1 (blue and red) cell lines and induction of RPL22L1 in the induced sgRPL22 cell lines compared to the NTC.

After sgRPL22L1-1 and sgRPL22L1-2 were introduced into the iPSCs, knockdown of RPL22L1 protein was observed (Figure 6C). Although both sgRNA exhibited potential leaky knockdown to some extent when compared to the NTC, similar to that of the sgRPL22-2, sgRPL22L1-2 was significantly more leaky in an uninduced environment. sgRPL22L1-1 decreased protein levels from about 0.5-fold with no TMP to 0.1-fold with TMP treatment, while that of sgRPL22L1-2 decreased from about 0.3-fold with no TMP to 0.2-fold with TMP treatment when compared to the NTC. Unlike the increased expression of RPL22L1 protein that was observed due to downregulation of RPL22, downregulation of RPL22L1 did not result in

increased expression of RPL22 (Figure 6B), indicating that compensation does not go both ways. These results validate that downregulation of RPL22 and RPL22L1 proteins in iPSCs can be achieved using our CRISPRi platform.

RNA expressions of RPL22 and RPL22L1 upon CRISPRi knockdown in iPSCs were also examined in addition to their protein expression (Figure 7). Both RPL22 sgRNAs significantly downregulated RPL22 RNA levels in comparison to that of the NTC (Figure 7A). In accordance with the observations in the western blot results, we also saw an induction of RPL22L1 upon RPL22 knockdown for both RPL22 sgRNAs (Figure 7B). Additionally, we detected a potential leaky knockdown of RPL22 and induction of RPL22L1 for sgRPL22-2 without TMP, once again confirming our findings from the protein analysis. With regards to the RPL22L1 sgRNAs, we only saw knockdown of RPL22L1 by sgRPL22L1-1, in addition to a potential leaky knockdown without TMP, which is analogous to our western blot results. We also noticed an upregulation of RPL22 RNA levels, as well as a leaky induction without TMP, as a result of RPL22L1 knockdown by sgRPL22L1-1 (Figure 7C), a result we did not see at the protein level. Looking at sgRPL22L1-2, we did not see successful knockdown of RPL22L1 (Figure 7D), therefore only sgRPL22L1-1 was used for further investigation. The validated cell lines with sgRPL22-1, sgRPL22-1, and sgRPL22L1-1 were then used to carry out further experiments to study how their downregulation may affect pluripotency genes and cell fate.

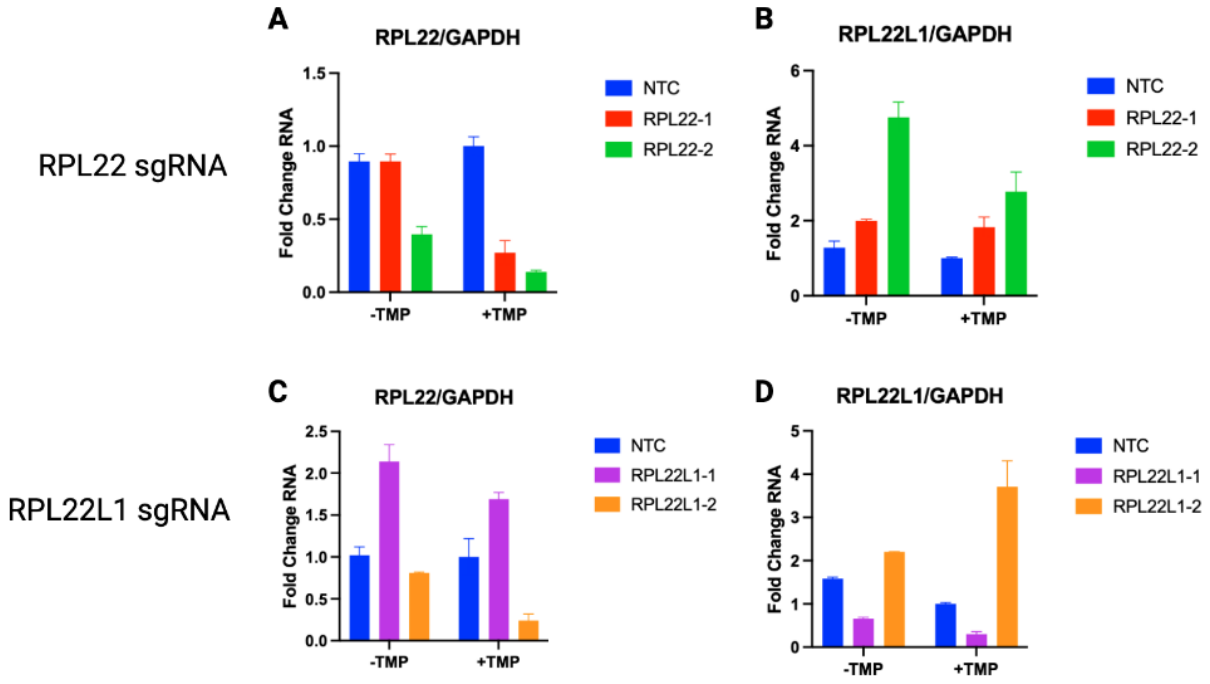

Figure 7: RNA analysis of RPL22 and RPL22L1 knockdown. (A) There is knockdown of RPL22 (B) and induction of RPL22L1 in both RPL22 sgRNAs (red and green) compared to the NTC (blue) at the RNA level. (C) There is knockdown of RPL22L1 in sgRPL22L1-1 (purple) but not sgRPL22L1-2 (orange) compared to the NTC. (D) There appears to be induction of RPL22 for sgRPL22L1-1 but not sgRPL22L1-2 compared to the NTC at the RNA level.

Downregulation of RPL22/RPL22L1 Does Not Affect the Expression of Pluripotency Genes

To study if the knockdown of RPL22 and RPL22L1 affect pluripotency of iPSCs, the RNA harvested from the sgRNA infected iPSC CRISPRi cells were used in a RT-qPCR experiment to measure the RNA changes of pluripotency markers. In the qPCR experiment, we looked at Pou5f1 (Oct4), SOX2, Nanog, and cMyc as markers of pluripotency. The RNA fold change for each marker was averaged across all replicates for each sgRNA, and the resulting data was graphed in Figure 8. When compared to the NTC, there was no significant difference in RNA fold change for SOX2, Nanog, and c-Myc when RPL22 and RPL22L1 were knocked down (Figure 8). There appears to be a moderate increase in Nanog expression due to RPL22L1 knockdown, however, we would want to conduct the experiment with another sgRNA for RPL22L1 to confirm this effect. In addition, we have also noticed a change in Pou5f1 expression

upon RPL22 and RPL22L1 knockdown. RPL22 knockdown slightly reduced the Pou5f1 expression, and RPL22L1 knockdown induced it, suggesting there could be a potential opposite regulation of Pou5f1 by RPL22 and RPL22L1. Taken in total, our data suggests that RPL22 and RPL22L1 may not play a significant role in global pluripotency expression, an assumption supported by normal cell morphology and proliferation observed during cell culture.

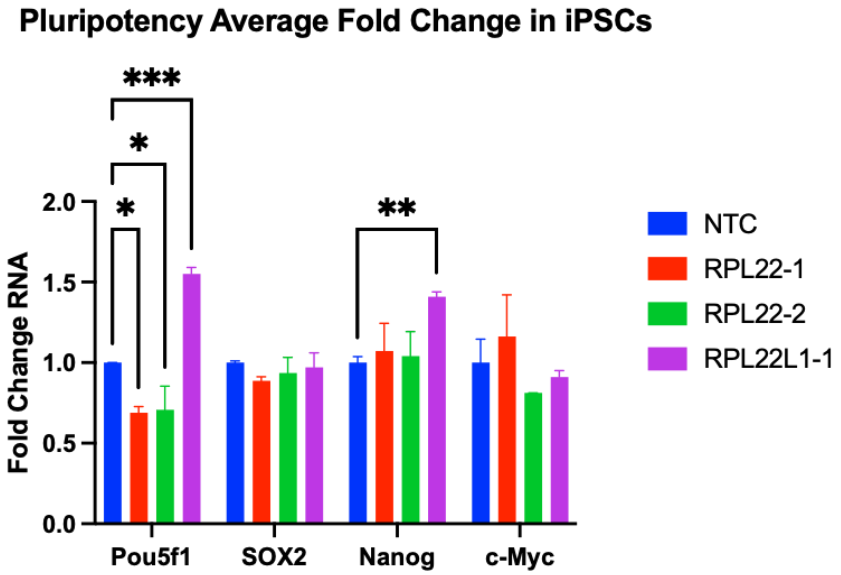

Figure 8: Pluripotency Average RNA Fold Change in iPSCs in RPL22 and RPL22L1 knockdown. Statistical analysis was done using a two-way ANOVA (P value: 0.0332 (*), 0.0021 (**), 0.0002 (***), <0.0001 (****). There was no significant difference in RNA fold change for SOX2, Nanog, and c-Myc when RPL22 (red and green) and RPL22L1 (purple) were knocked down compared to the NTC (blue). However, RPL22 knockdown slightly reduced Pou5f1 expression and RPL22L1 knockdown induced it.

Overall, these findings demonstrate that RPL22 and RPL22L1 knockdown in iPSCs does not affect the global expression of pluripotency markers, suggesting their knockdown does not affect the maintenance of iPSCs at pluripotency state. Since the pluripotency of the cells remains unaffected, we then studied whether the knockdown of RPL22 and RPL22L1 affects the differentiation of iPSCs.

Downregulation of RPL22L1 Resulted in Defect in EB Formation

In order to investigate the effects of RPL22 and RPL22L1 knockdown in iPSC differentiation, embryoid bodies (EBs) were used. EBs are three-dimensional cell aggregates containing the structure of early embryos and cells of all three germ layers[13]. Therefore, the iPSC-derived EBs could serve as an *in vitro* differentiation model system to study roles of RPL22 and RPL22L1 in cell differentiation and fate determination. The validated CVB-iPSC CRISPRi lines with RPL22 and RPL22L1 knockdown, as well as the line with NTC, were used to generate EBs. On day 1 of EB formation, half of the EBs for each line were treated with TMP to induce the downregulation of RPL22 and RPL22L1, while the other half remained untreated as a control. The induced EBs were treated with TMP throughout the entire experiment.

At the iPSC stage, the blue fluorescent signal in the sgRNA constructs of both NTC and RPL22L1 sgRNAs can be detected in all the cells (Figure 9A). This indicates high infection efficiency and successful expression of the sgRNAs in the iPSCs. On day 7 and day 14 of EB formation, knockdown of RPL22L1 in EBs exhibited abnormal EB morphology (Figure 9B, bottom left panel). On day 7, the EBs with RPL22L1 knockdown had an average diameter of about 24.5 μm, making them almost 40% smaller than the EBs with NTC sgRNA. On day 14, while the EBs with NTC sgRNA grew to about 57 μm in diameter, that of the RPL22L1 sgRNA shrunk to only an average of 14 μm in diameter, making them about 75% smaller than the NTC EBs. In addition to the RPL22L1 EBs being significantly smaller than the NTC control at both time points, although they were relatively spherical, their surfaces were much more rough and uneven rather than smooth. After day 14, EBs with RPL22L1 sgRNA continued to shrink and were unable to be collected and used for RNA analysis.

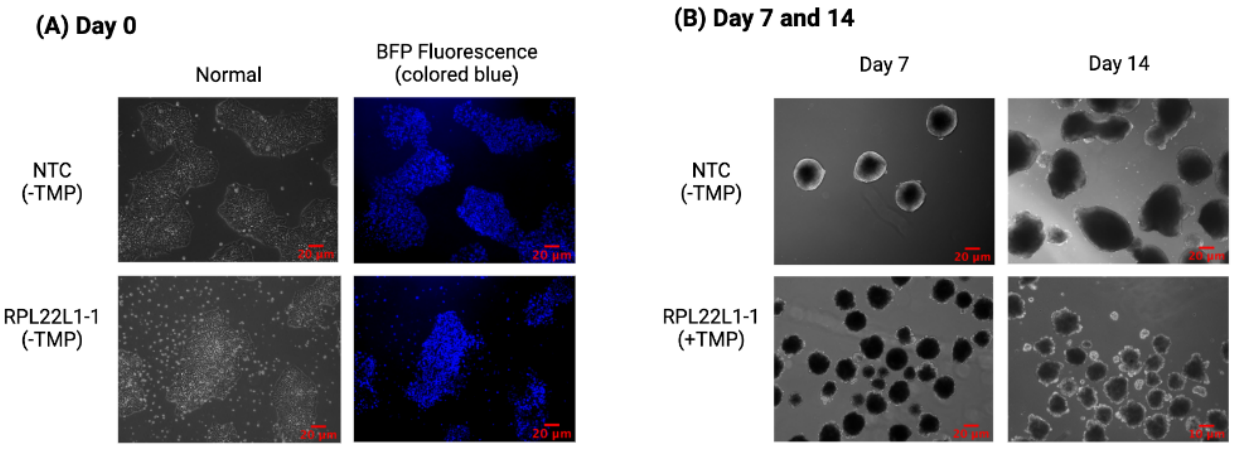

Figure 9: iPSC and EB images of NTC and RPL22L1 knockdown at day 0, 7, and 14. (A) Day 0 images of CVB iPSC cells containing sgNTC (top row) and sgRPL22L1-1 (bottom row) in normal (left column) and BFP fluorescence (colored blue) (right column) imaging. (B) Day 7 and 14 images of NTC EBs (top row) and RPL22L1 knockdown EBs with sgRPL22L1-1 (bottom row).

Capturing images of the EBs at various time points allowed us to track the progression of EB formation and growth. Due to the lack of growth, abnormal morphology, and eventual death of the sgRPL22L1-1 EBs, we believe the RPL22L1 may be essential for cell survival and embryonic development, supporting the idea in previous publications that RPL22L1 knockdown impairs cell growth, and its knockout is embryonic lethal[4,12].

Downregulation of RPL22 Effects Cell Lineage Marker Expression

Given that RPL22L1 knockdown caused unhealthy EB formation, we then focused on studying the effects of RPL22 knockdown in iPSC differentiation. Throughout iPSC maintenance and EB formation, the cells from the NTC control, sgRPL22-1, and sgRPL22-2 were harvested on day 0, the day the iPSCs were dissociated for EB formation, and day 7, 14, and 21 after EB formation, and used for RNA analysis. The harvested RNA samples were used to perform reverse transcription polymerase chain reaction (RT-PCR) to synthesize cDNA. The cDNA was then utilized in quantitative PCR (qPCR) with primers targeting various ribosomal proteins, pluripotency, and differentiation markers of the three germ layers (Table 2) to determine

the changes of each marker during differentiation in each cell line. The results generated from the qPCR analysis were then used to determine whether knockdown of RPL22 affected the expression of other ribosomal proteins and the differentiation of the three germ layers.

Ribosomal Proteins

In addition to analyzing the knockdown efficiency of the two RPL22 sgRNAs in iPSCs and throughout differentiation at the RNA level, we also examined the RNA expression of select ribosomal proteins, RPL36AL and RPL10A, in each cell line to determine whether knockdown of RPL22 has an effect on other ribosomal proteins. Our qPCR analysis confirmed our findings from our protein analysis. It showed a successful knockdown of RPL22 which resulted in upregulation of RPL22L1 (Figure 10A-B), suggesting the compensation of RPL22 reduction by RPL22L1 is not only at the protein level but also at the RNA level. In addition, RPL22 knockdown did not significantly affect the expression of RPL36AL and RPL10A at all time points, indicating that decreased RPL22 expression does not affect the selected ribosomal proteins. There might be a potential upregulation of RPL36AL due to RPL22 knockdown at day 21, however further experiments are needed to solidify this finding. Further, more experiments might also be needed to evaluate the global effects of RPL22 knockdown on all ribosomal proteins. We also noticed from the NTC control line that RPL22 and RPL10A RNA levels increased over time as the cells differentiated (Figure 10A, D), but that of RPL22L1 and RPL36AL did not (Figure 10B, C), which demonstrates that the dynamics of ribosomal protein expression patterns are not all the same during stem cell differentiation.

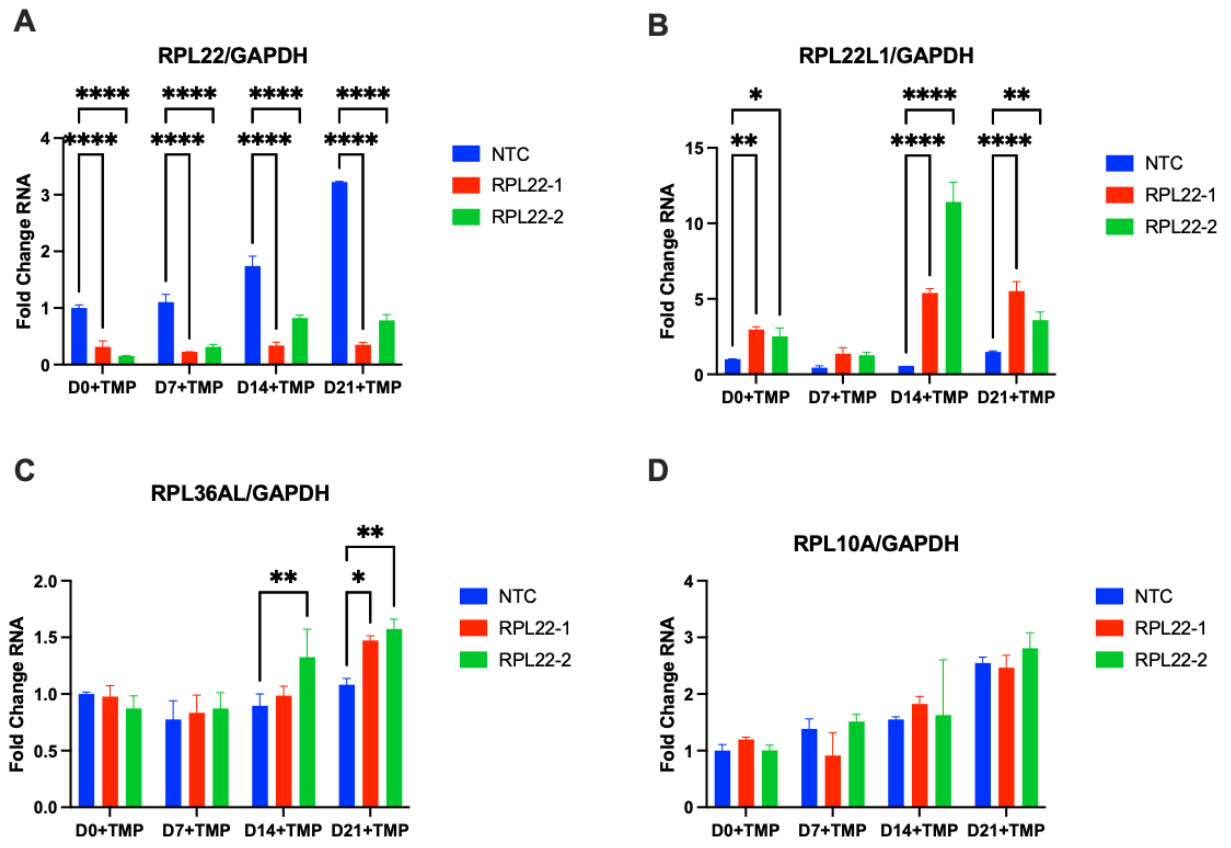

Figure 10: Graphs of RNA fold change of ribosomal proteins in RPL22 knockdown EBs over time. The RNA levels of the ribosomal proteins were normalized to GAPDH. Fold change was calculated relative to the amount in NTC. Statistical analysis was done using a two-way ANOVA (P value: 0.0332 (*), 0.0021 (**), 0.0002 (***), <0.0001 (****). (A) RNA fold change of RPL22 - there is downregulation of RPL22 expression. (B) RNA fold change of RPL22L1 - there is induction of RPL22L1 expression. (C) RNA fold change of RPL36AL - there is no change in RPL36AL expression. (D) RNA fold change of RPL10A - there is no change in RPL10A expression.

Pluripotency Markers

As mentioned above, knockdown of RPL22 does not affect pluripotency markers in iPSCs. However, the effects of RPL22 knockdown on the pluripotency markers during iPSC differentiation into embryoid bodies still remained unknown. Therefore, the RNA expression of pluripotency markers, Pou5F1 (Oct4), Nanog, and c-Myc, were examined by qPCR. Our results demonstrated that the RNA levels of Pou5f1, Nanog, and c-Myc in the NTC were relatively high in iPSCs, followed by a substantial decrease in expression during EB formation and growth

(Figure 11A-C). The trends of reduction of the pluripotency markers are similar to the previous publications[14,15]. Knockdown of RPL22 with two different sgRNAs did not significantly affect the expression of these pluripotency markers in EBs at all time-points. Similar to our previous results, we saw downregulation of Pou5f1 due to RPL22 knockdown on day 0 prior to EB formation, however this decreased expression did not persist after EB formation, suggesting that RPL22 may only affect Pou5f1 expression in iPSCs (Figure 11A). These results explicitly show that knockdown of RPL22 does not affect the expression of pluripotency genes during differentiation.

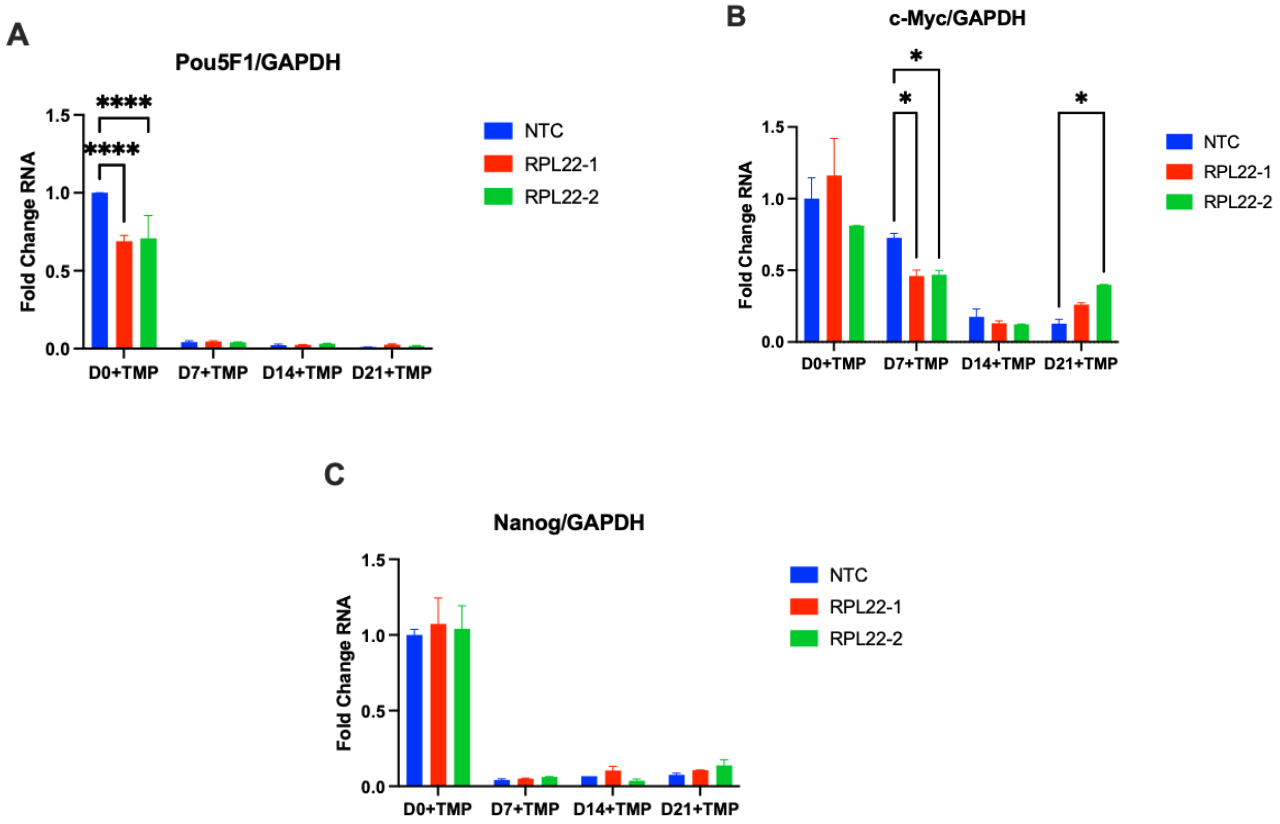

Figure 11: Graphs of RNA fold change of pluripotency markers in RPL22 knockdown EBs over time. The RNA levels of the pluripotency markers were normalized to GAPDH. Fold change was calculated relative to the amount in NTC. Statistical analysis was done using a two-way ANOVA (P value: 0.0332 (*), 0.0021 (**), 0.0002 (***), <0.0001 (****). (A) RNA fold change of Pou5F1 - there is no change in Pou5F1 expression. (B) RNA fold change of Nanog - there is no change in Nanog expression. (C) RNA fold change of c-Myc - there is no change in c-Myc expression.

Endoderm Differentiation Markers

The next portion of differentiation markers we analyzed were markers for the three germ layers: endoderm, mesoderm, and ectoderm. These germ layers develop during early embryonic development and give rise to all cells of the body, so understanding how they are affected by RPL22 downregulation could further our understanding of the role RPL22 plays on early embryonic cell fate determination.

GATA4 and GATA6 are classical markers of endoderm differentiation, however, our qPCR data revealed large RNA expression variations for both genes, preventing us from discerning any trend. Additional experiments are needed in order to get better amplification of both markers for a more accurate analysis. Despite this lack of data for GATA4 and GATA6, we were able to observe trends in CXCR4 and WNT3 (Figure 12). There is a significant upregulation of both CXCR4 and WNT3 on days 14 and 21 on the account of RPL22 knockdown. Our data suggests that RPL22 may affect the expression of select endoderm markers.

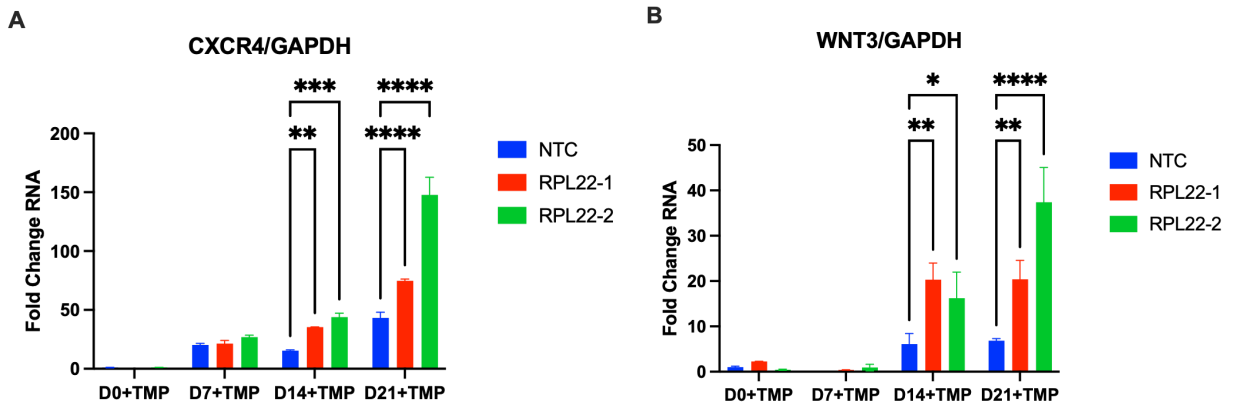

Figure 12: Graphs of RNA fold change of endoderm markers in RPL22 knockdown EBs over time. The RNA levels of the endoderm markers were normalized to GAPDH. Fold change was calculated relative to the amount in NTC. Statistical analysis was done using a two-way ANOVA (P value: 0.0332 (*), 0.0021 (**), 0.0002 (***), <0.0001 (****). (A) RNA fold change of CXCR4 - there is induction of Pou5F1 expression. (B) RNA fold change of WNT3 - there is induction of WNT3 expression at day 14 but the same trend is not observed at any other time points.

Mesoderm Differentiation Markers

To evaluate the effect of RPL22 on mesodermal differentiation, the mesoderm differentiation markers T, PDGFRA, KDR, BMP4, and p53 were examined. Our qPCR results revealed that the RNA expression of T, KDR, and p53 did not appear to be affected by knockdown of RPL22 as no significant changes can be seen across multiple time points for both sgRNAs (Figure 13A, C, E). There appears to be a moderate increase in expression of p53 on day 21, however, the upregulation is not nearly as significant as that found for PDGFRA and BMP4 on the same day (Figure 13E). Both PDGFRA and BMP4 RNA levels were significantly increased as a result of RPL22 knockdown when compared to the control (Figure 13B, D). This trend is clearly seen in Figures 13B and D on days 14 and 21, specifically. Our results of the mesoderm markers indicate that not all mesoderm genes are influenced by RPL22. However, RPL22 may affect the expression of a subset of mesoderm markers at later stages of EB differentiation, suggesting that RPL22 is important for the differentiation or maturation of specific mesoderm-derived cell types.

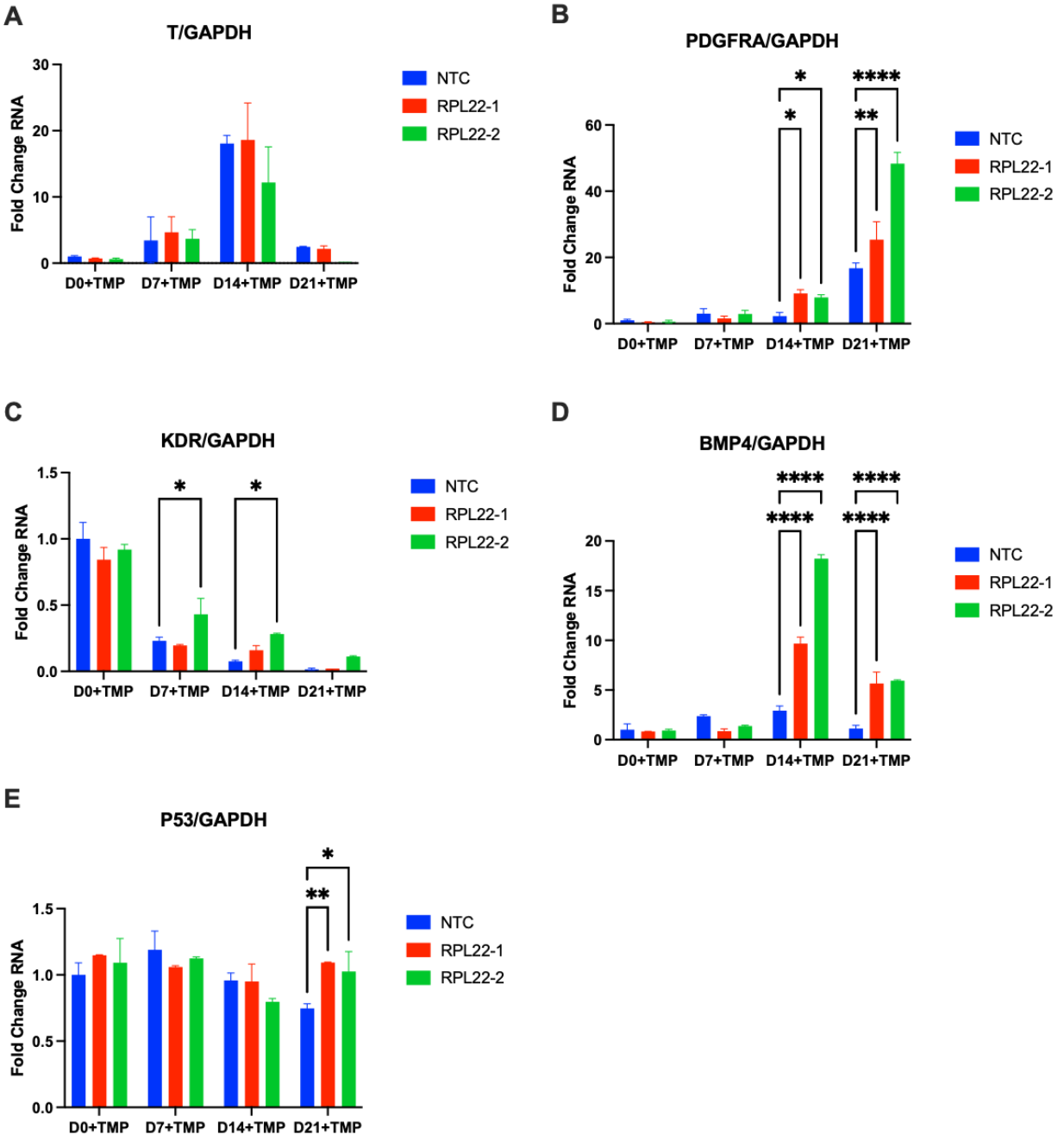

Figure 13: Graphs of RNA fold change of mesoderm markers in RPL22 knockdown EBs over time. The RNA levels of the mesoderm markers were normalized to GAPDH. Fold change was calculated relative to the amount in NTC. Statistical analysis was done using a two-way ANOVA (P value: 0.0332 (*), 0.0021 (**), 0.0002 (***), <0.0001 (****). (A) RNA fold change of T - there is no change in T expression. (B) RNA fold change of PDGFRA - there is induction of PDGFRA expression. (C) RNA fold change of KDR - there is no change in KDR expression. (D) RNA fold change of BMP4 - there is induction of BMP4 expression. (E) RNA fold change of p53 - there is no change in p53 expression.

Ectoderm Differentiation Markers

To examine the role of RPL22 on ectoderm differentiation, we analyzed the following ectoderm differentiation markers: SOX1, STMN2, Nestin, NeuroD1, and FABP7. Similar to the mesoderm genes, only some of the ectoderm genes were affected by RPL22 knockdown. There was no significant change on the RNA expression of Nestin and FABP7 upon RPL22 knockdown when compared to the NTC control (Figures 14C and E). SOX1 did not exhibit any significant change on day 0 to day 14 under RPL22 knockdown, however, a moderate but significant reduction was observed on day 21 (Figure 14A). Neuron markers STMN2 and NeuroD1 both demonstrated substantial downregulation in comparison to the control on day 21 when RPL22 was knocked down (Figure 14B, and D). We can deduce that some, but not all, ectoderm markers are impacted by RPL22 knockdown. We speculate that RPL22 may affect a small subset of cell lineages within the ectoderm, but further investigation is needed to determine what these cell types are. Given that SOX1 and Nestin are neuron progenitor markers, FABP7 is expressed in neural stem cells and astrocytes, and STMN2 and NeuroD1 are expressed in the later stage of neuron differentiation as immature neuron markers, our data suggests that RPL22 may not affect the neuron progenitor formation but may specifically affect the terminal differentiation of neurons.

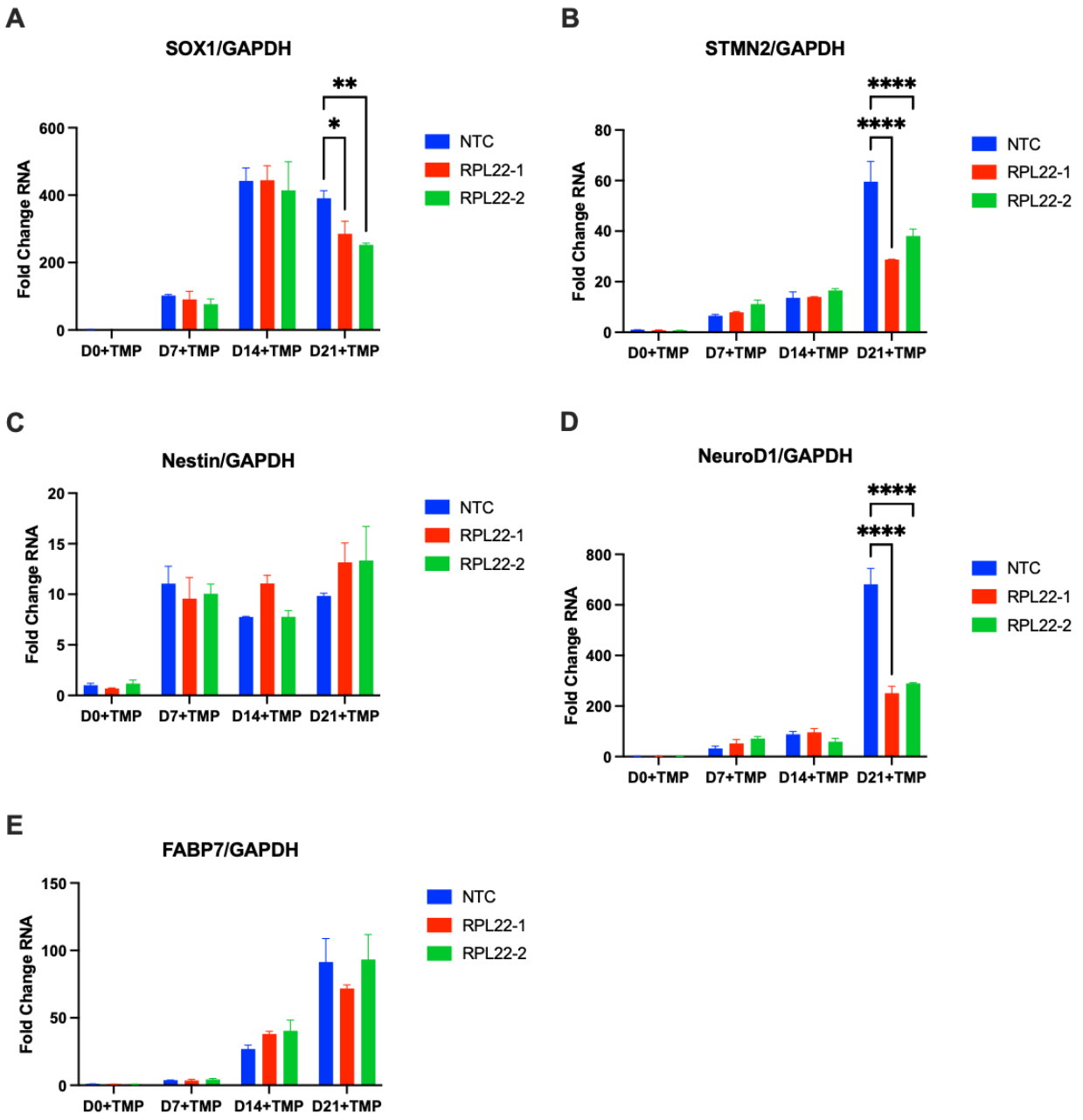

Figure 14: Graphs of RNA fold change of ectoderm markers in RPL22 knockdown EBs over time. The RNA levels of the ectoderm markers were normalized to GAPDH. Fold change was calculated relative to the amount in NTC. Statistical analysis was done using a two-way ANOVA (P value: 0.0332 (*), 0.0021 (**), 0.0002 (***), <0.0001 (****). (A) RNA fold change of SOX1 - there is downregulation of SOX1 expression. (B) RNA fold change of STMN2 - there is downregulation of STMN2 expression. (C) RNA fold change of Nestin - there is no change in Nestin expression. (D) RNA fold change of NeuroD1- there is downregulation of NeuroD1 expression. (E) RNA fold change of FABP7 - there is no change in FABP7 expression.

In summary, our qPCR data revealed that knockdown of RPL22 does not have an effect on pluripotency and select ribosomal proteins. However, it does influence certain genes within each of the three germ layers, while other genes remain unaffected. We discovered that a small subset of mesoderm and endoderm differentiation markers are increased as a result of RPL22 knockdown, while some markers in the ectoderm layer are decreased. Determining the specific cell lineages within each germ layer that are directly affected by the downregulation of RPL22 will require additional exploration, but these preliminary results could guide our future experimentation toward uncovering precisely which cell types are impacted.

Generation of APOBEC1-RPL22 and RPL22L1 fusion constructs

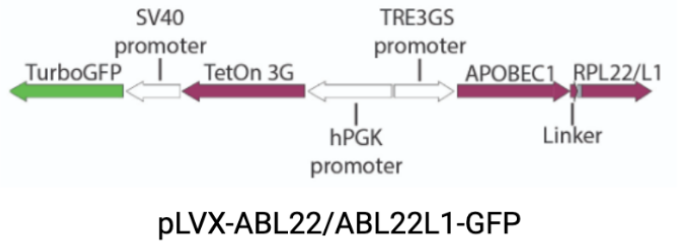

Figure 15: Diagram of the APOBEC-RPL22/L1 fusion protein construct. APOBEC1-RPL22 or APOBEC1-RPL22L1 gene fragment was first inserted into the pLVX plasmids under the control of a tetracycline-responsive element promoter**.**

Given that our results and previous publications demonstrated that RPL22 and its paralog RPL22L1 may have distinct functions in the regulation of early embryonic development and cell differentiation, we are interested in investigating whether they affect the translation of different subset of genes or have different RNA targets. To study this question, a recent technology, STAMP (Surveying Targets by APOBEC Mediated Profiling), developed in the lab was adapted[10]. In brief, RPL22, RPL22L1, or any RNA-binding protein of interest is fused to the cytidine deaminase enzyme APOBEC1, which mediates C-to-U editing on single-stranded RNAs. Therefore, when the fusion protein is overexpressed in the cells, it could guide the

APOBEC1 to convert the Cs to Us in the proximal of its binding sites which allows us to identify the binding sites of the proteins of interest by performing RNA sequencing. To overexpress the APOBEC1-RPL22 and -RPL22L1 fusion proteins in the cells, a synthesized APOBEC1-RPL22 or APOBEC1-RPL22L1 gene fragment was first inserted into the pLVX plasmids under the control of a tetracycline-responsive element promoter, which allows us precise control of the expression of APOBEC1 fusion protein (Figure 15). Next, to confirm the integration of the construct in the cells and to easily select the cells via FACS sorting, the puromycin-resistant gene in the original plasmid was replaced by a TurboGFP. The lentivirus of APOBEC1-RPL22 and APOBEC1-RPL22L1 were generated and used to successfully transduce the CVB-iPSCs, as indicated by the visible green fluorescence (Figure 16). Further experiments are needed to determine if the constructs work to identify and distinguish the differences of the RNA binding targets of RPL22 and RPL22L1.

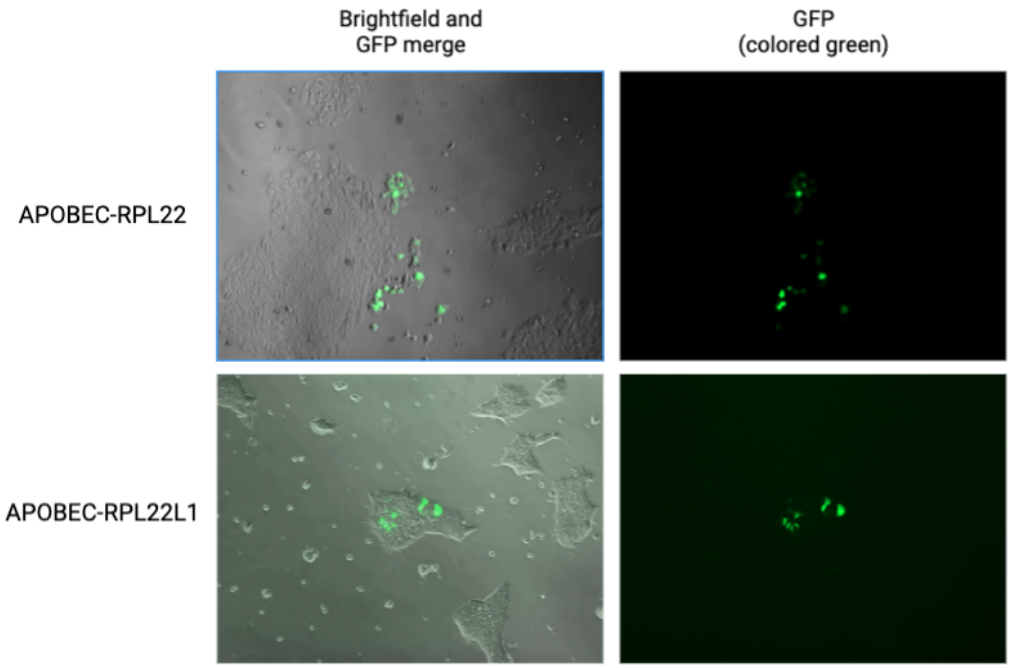

Figure 16: Images of CVB-iPSC cells with APOBEC-RPL22 (top row) and APOBEC-RPL22L1 (bottom row) fusion constructs. Both transduced cells emit fluorescence, indicating successful expression of our construct.

DISCUSSION

To investigate early cell fate determination as a result of RPL22 and RPL22L1 knockdown using the CRISPRi system, we employed an iPSC differentiation model. To ensure the effectiveness of our sgRNAs for both ribosomal proteins, we conducted protein and RNA analysis to confirm knockdown of RPL22 and RPL22L1 in our cells. We then studied whether RPL22 and RPL22L1 affected the expression of pluripotency genes to confirm that our iPSCs were still able to be maintained at the pluripotency state. Once this step was completed, we used our validated RPL22 and RPL22L1 knockdown lines to perform EB formation assay in order to investigate their roles in early embryonic differentiation. Finally, we generated APOBEC1-RPL22 and -RPL22L1 fusion constructs in preparation for determining the translational targets of these ribosomal proteins. Taken in combination, we hope to gain insight into which cell fates RPL22 and RPL22L1 may play a role in and the mechanism behind their regulation.

We began our study by introducing RPL22 and RPL22L1 sgRNAs into the CVB-iPSC CRISPRi line and conducting protein and RNA analysis to confirm knockdown of the corresponding proteins. At both the protein and RNA level, we observed significant downregulation of RPL22 in both sgRNA-infected cells. In those same cell lines, we also noticed an induction of RPL22L1, a result that coincides with the findings of a previous study conducted by O'Leary et al[12]. They found a compensatory increase in RPL22L1 in RPL22 -/- mice. Further, they determined that RPL22 binds to an internal hairpin structure within RPL22L1 mRNA, thereby repressing its expression[12]. Our results support the idea that the compensation of RPL22 by RPL22L1 can also be seen in human developmental models. Interestingly, when RPL22L1 was knocked down, the same compensatory effect was not seen in RPL22 at the protein level,

but it was observed at the RNA level for one of the RPL22L1 sgRNA. Given that only one of the RPL22L1 sgRNA can effectively downregulate both RNA and protein levels of RPL22L1, more sgRNAs and experiments are needed to test if our observations are repeatable. Additionally, since RPL22L1 compensates for the loss of RPL22, but RPL22 does not compensate for the reduction of RPL22L1, this demonstrates that these two proteins may play different functions in the cells.

In addition to the compensatory regulation between RPL22 and RPL22L1, it would be interesting to test if RPL22 or RPL22L1 affect the expression of other ribosomal proteins and further affect the ribosome stoichiometry. Select ribosomal proteins, RPL10A and RPL36AL, were tested, and it appears that knockdown of RPL22 did not significantly affect the RNA expression of select ribosomal proteins in iPSCs and EBs. These results suggest RPL22 downregulation may specifically induce the expression of RPL22L1, but not the other ribosomal proteins. Further studies may be needed to test if RPL22 affects the expression of the rest of ribosomal proteins and also if the increased RPL22L1 replaces the RPL22 binding site on the ribosome complex upon RPL22 knockdown. For RPL22L1, its knockdown significantly affected the EB formation which prevented us from collecting enough material for further analysis. Therefore, the effect of RPL22L1 on other ribosomal proteins will be examined by other methods in the future.

To study the role of RPL22 and RPL22L1 in early embryonic cell fate determination, we first examined how they affect iPSC pluripotency. Maintaining pluripotency in iPSCs is essential for self-renewal and their ability to differentiate into the three germ layers, mesoderm, endoderm, and ectoderm. In the context of RPL22 and RPL22L1 knockdown in iPSCs, we did not notice

any morphological change of iPSC colonies (data not shown). We further used a qPCR experiment to analyze the RNA changes of Pou5F1, SOX2, Nanog, and c-Myc, all of which are classical pluripotency transcription factors, and none of their expressions were significantly altered by RPL22 knockdown during EB formation. We did notice downregulation of Pou5f1 due to RPL22 knockdown and induction due to RPL22L1 knockdown in iPSCs, however it did not seem to affect the cells' ability to differentiate. Our results suggest downregulation of RPL22 and RPL22L1 does not affect the global maintenance of iPSC at the pluripotency state, and does not trigger spontaneous differentiation of iPSCs before performing EB formation.

To study how RPL22 and RPL22L1 affects cell fates, we investigated how the expression of mesoderm, endoderm, and ectoderm differentiation markers changed as a result. For the EBs with RPL22L1 knockdown by sgRPL22L1-1, an abnormally small and misshapen morphology with rough surfaces was observed. Instead of growing larger over time, RPL22L1 knockdown EBs actually shrunk from day 7 to 14. Following day 14, all the RPL22L1 knockdown EBs continued to shrink and eventually died, which suggests that RPL22L1 is essential for cell proliferation and embryonic development. This is somewhat consistent with a previous study done by Zhang et al. in 2017 that explored how RPL22 and RPL22L1 control morphogenesis[4]. They found that RPL22L1-/- mouse embryos were abnormal 9.5 days post-coitus and completely absent 12 days post-coitus, thereby concluding that RPL22L1 deficiency is embryonic lethal[4]. Our results support their findings with regards to RPL22L1 being an essential ribosomal protein. Compared to the RPL22L1 knockdown EBs, RPL22 knockdown EBs, by both of the sgRNAs, were able to grow until completion of the experiment on day 21, and were able to be used further in RNA analysis. It has also been shown in previous studies that RPL22 and RPL22L1 play antagonistic regulatory functions in hematopoiesis in zebrafish and mice[3,16,17]. Our results

provide further evidence that RPL22 and its paralog RPL22L1 may play distinct functions in cell proliferation and cell fate determination.

As RPL22 did not affect the expression of pluripotency markers in iPSCs and EBs, its effects on EB differentiation were accessed. Similar to embryos, EBs contain cells of all three germ layers, endoderm, mesoderm, and ectoderm, which give rise to all the organs and tissues that will make up the organism. The innermost layer, the endoderm, and the outermost layer, the ectoderm, interact to form the mesoderm, or middle layer[18]. Cells within the endoderm mature to form the epithelium, digestive tract, liver, pancreas, and lungs[19]. The mesoderm also helps give rise to the digestive tract, but also forms the heart and skeletal muscles, red blood cells, tubules of the kidneys, and connective tissue (mesenchyme)[20]. Lastly, the ectoderm differentiates into two parts - the surface ectoderm and the neuroectoderm which is crucial for neurulation or the development of the nervous system. The surface ectoderm matures into the outer surfaces of the body such as the epidermis, hair, and nails. The neuroectoderm further differentiates into the neural tube, which later forms the central nervous system, and the neural crest which forms parts of the peripheral nervous system[21]. The differentiation markers we explored encourage cells to differentiate toward these lineages, so understanding how they might be affected due to RPL22 knockdown can give us insight into how RPL22 may be involved in determining cell fate.

We began our investigation by looking at the endoderm differentiation markers. Despite RNA levels being too low for GATA4 and GATA6, two markers traditionally used for early endoderm detection, to distinguish any trend in expression, we focused our attention on CXCR4 and WNT3. CXCR4 is an important marker of the definitive endoderm which later develops into the respiratory system and digestive tract[22,23]. It was also found to be an essential gene given that its knockout in mice leads to embryonic lethality[24]. When RPL22 was knocked down in our EBs,

a substantial increase in CXCR4 expression was observed, suggesting that RPL22 may play a regulatory role in definitive endoderm differentiation. In addition, induction of WNT3 expression upon RPL22 knockdown was also observed. WNT3 is another important marker of the definitive endoderm. It was found that its mRNA levels could be used to predict definitive endoderm differentiation efficiency such that WNT3 overexpression promotes differentiation[25]. Together, our studies suggest that RPL22 contributes to definitive endoderm formation and the development of its derivative cell types, such as the digestive tract and hepatocytes.

For the analysis of the mesoderm germ layer, we investigated the RNA levels of T, PDGFRA, BMP4, p53, and KDR. The T gene, or Brachyury, is an early mesoderm marker that plays an important role in mesoderm formation and organization. It was found to be an essential gene for embryonic survival when studied in T-/- mice[26]. From our results, we did not observe any significant change on T when knocking down RPL22, suggesting RPL22 may not be involved in the regulation of early mesoderm commitment. KDR was another gene that was unaffected by RPL22 knockdown. KDR is also an early mesoderm marker, and a previous study using human embryonic-stem-cell-derived EBs had used KDR as a marker of cardiovascular progenitors given its presence in cardiac, endothelial, and vascular smooth muscle cells[27,28]. Given that we saw no change in KDR expression as a result of RPL22 knockdown, this supports the idea that RPL22 does not influence early mesoderm cell fate. Another mesoderm marker that we found was not affected by RPL22 knockdown was p53, a gene that is typically known as a tumor suppressor. However, a study found that the p53 family is also essential for early mesoendoderm differentiation of pluripotent cells in embryos, again supporting our findings that RPL22 does not affect early mesoderm development[29]. To note, p53 is a known target gene of RPL22 given RPL22's ability to activate p53 in tumor suppression research, however, this

interaction takes place at the protein level whereas our data analyzes the interaction of RPL22 and p53 and the RNA level[30].

Two mesoderm cell lineage differentiation markers that were significantly impacted by RPL22 knockdown were PDGFRA and BMP4. PDGFRA is a mesoderm marker whose expression was found to support differentiation into mesenchymal stem cells and myofibroblasts, while BMP4 is an essential marker for hematopoietic differentiation[31,32]. We noticed knockdown of RPL22 affected PDGFRA and BMP4 RNA expression at the later time-points of EB formation, suggesting RPL22 may affect the commitment or differentiation of specific mesoderm-derived cell types that express PDGFRA and BMP4, such as the hematopoietic lineage. This echoes previous studies that RPL22 plays an important role in regulating hematopoietic stem cell maintenance and differentiation[3,16,17].

For the third and final germ layer, the ectoderm differentiation markers we investigated were SOX1, STMN2, Nestin, NeuroD1, and FABP7. SOX1, Nestin, and FABP7 are early ectoderm markers. In a previous study, it was found that SOX1 is one of the earliest markers of ectoderm cells that are committed to a neural fate[33]. Nestin is another classical marker for neural progenitor cells of the neuroectoderm, and FABP7 is a marker of radial glial cells which are crucial for the migration of neural progenitor cells[34,35]. Nestin and FABP7 do not exhibit change in expression due to RPL22 knockdown, while SOX1 expression appears to be slightly reduced on day 21. Similarly, STMN2 and NeuroD1 also showed downregulation as a result of RPL22 knockdown. Both of these genes are known to be immature and mature neuronal markers, which supports their late increase in expression that is seen in our data. STMN2 promotes the differentiation of motor neurons while NeuroD1 drives neurogenesis and neuronal migration[36,37]. In summary, we speculate that RPL22 may not affect the early ectoderm commitment and the

differentiation to most of the neural lineages, but may play a specific role in regulating neuron differentiation and maturation.

To identify the binding targets of RPL22 and RPL22L1, we will use our synthesized STAMP constructs, APOBEC-RPL22 and -RPL22L1 fusion proteins, in future experiments. In our transduced CVB-iPSCs, we plan to induce overexpression of the fusion protein and differentiate the cells into EBs to study their effects during early embryonic development. Alternatively, we could differentiate the cells into specific cell types to study how RPL22 and RPL22L1 influence certain cell lineages. In either case, we will employ bulk and single-cell RNA-seq to identify the translational and RNA binding targets of RPL22 and its paralog, RPL22L1. These results will reveal which subsets of genes or RNA they regulate and how they differ from one another.

CONCLUSION AND FUTURE DIRECTIONS

My Thesis demonstrates an effective CRISPRi system, with accompanying sgRNAs, in an iPSC differentiation model that allows for the investigation of RPL22 and RPL22L1 influence on early cell fate determination. We found that both RPL22 and RPL22L1 do not regulate pluripotency nor other ribosomal proteins. Our results suggest that RPL22L1 is an essential protein for cell survival, as supported by previous studies. We also found that RPL22 regulates various cell fates in each of the three germ layers, however more experiments are needed to determine exactly which cell lineages are affected and the mechanism behind their regulation. In terms of endoderm differentiation, we found upregulation of CXCR4 and possibly WNT3 as a result of RPL22 knockdown, suggesting that RPL22 may contribute to definitive endoderm development. Downregulation of RPL22 induced expression of PDGFRA and BMP4 mesoderm markers, indicating that RPL22 may affect the differentiation of mesoderm-derived cell types, such as hematopoietic stem cells and smooth muscle cells. Lastly, we discovered that RPL22 may play a role in neuron differentiation due to significant changes observed in STMN2 and NeuroD1 ectoderm marker expressions. To conclude this study, we successfully generated APOBEC-RPL22 and -RPL22L1 fusion constructs to use in future experiments to identify the translational and non-translation targets of both ribosomal proteins in the hopes of gaining insight into the exact cell lineages they may regulate.

Although this thesis provides preliminary evidence that RPL22 contributes to numerous cell fates, further investigation is needed to build a more robust layout of its specific regulatory targets. For example, the same experiment workflow could be conducted in a CRISPR activation (CRISPRa) system to determine if overexpression of RPL22 and RPL22L1 will have the opposite effects. Additionally, since we found that RPL22 may influence neuron differentiation,

another future experiment could be modulating RPL22 expression during differentiation of iPSCs into neurons, and studying the effects. The APOBEC-RPL22 and -RPL22L1 fusion constructs generated in this study can also be used in STAMP to determine the exact translational and even non-translation targets of both proteins.

This thesis lays the groundwork for further exploration into the regulatory targets of ribosomal proteins. Since it has been discovered that ribosomes have heterogeneity, it is crucial that we study the regulatory roles of ribosomal proteins both within the ribosome and out. Gaining a more robust understanding of each individual ribosomal protein will strengthen our knowledge about cell growth, differentiation, and maturation.

REFERENCES

1. Genuth, N. R. & Barna, M. The discovery of ribosome heterogeneity and its implications for gene regulation and organismal life. *Molecular Cell* **71**, 364–374 (2018).

2. Shi, Z., Fujii, K., Kovary, K. M., Genuth, N. R., Röst, H. L., Teruel, M. N. & Barna, M. Heterogeneous ribosomes preferentially translate distinct subpools of mrnas genome-wide. *Molecular Cell* **67**, (2017).

3. Zhang, Y., Duc, A. E., Rao, S., Bilbee, A. N., Rhodes, M., Li, Q., Kappes, D. J., Rhodes, J. & Weist, D. L. Control of hematopoietic stem cell emergence by antagonistic functions of ribosomal protein paralogs. *Developmental Cell* **24**, 411–425 (2013).

4. Zhang, Y., O'Leary, M. N., Peri, S., Wang, M., Zha, J., Melov, S., Kappes, D. J., Feng, Q., Rhodes, J., Amieux, P. S., Morris, D. R., Kennedy, B. K. & Weist, D. L. Ribosomal proteins RPL22 and RPL22L1 control morphogenesis by regulating pre-mrna splicing. *Cell Reports* **18**, 545–556 (2017).

5. Huang, F. & Chen, Y.-G. Regulation of TGF-β receptor activity. *Cell & Bioscience* **2**, 9 (2012).

6. Larson, M. H., Gilbert, L. A., Want, X., Lim, W. A., Weissman, J. S. & Qi, L. S. CRISPR interference (CRISPRI) for sequence-specific control of gene expression. *Nature Protocols* **8**, 2180–2196 (2013).

7. Gilbert, L. A., Horlbeck, M. A., Adamson, B., Villalta, J. E., Chen, Y., Whitehead, E. H., Guimaraes, C., Panning, B., Ploegh, H. L., Bassik, M. C., Qi, L. S., Kampmann, M. & Weissman, J. S. Genome-scale CRISPR-mediated control of gene repression and activation. *Cell* **159**, 647–661 (2014).

8. Tian, R., Gachechiladze, M. A., Ludwig, C. H., Laurie, M. T., Hong, J. Y., Nathaniel, D., Prabhu, A. V., Fernandopulle, M. S., Patel, R., Abshari, M., Ward, M. E. & Kampmann, M. CRISPR interference-based platform for multimodal genetic screens in human ipsc-derived neurons. *Neuron* **104**, (2019).

9. Zhang, R., Xu, W., Shao, S. & Wang, Q. Gene silencing through CRISPR interference in bacteria: Current advances and future prospects. *Frontiers in Microbiology* **12**, (2021).

10. Brannan, K. W., Chaim, I. A., Marina, R. J., Yee, B. A., Kofman, E. R., Lorenz, D. A., Jagannatha, P., Dong, K. D., Madrigal, A. A., Underwood, J. G. & Yeo, G. W. Robust single-cell discovery of RNA targets of RNA-binding proteins and ribosomes. *Nature Methods* **18**, 507–519 (2021).

11. Salter, J. D., Bennett, R. P. & Smith, H. C. The APOBEC protein family: United by structure, Divergent in function. *Trends in Biochemical Sciences* **41**, 578–594 (2016).

12. O'Leary, M. N., Schreiber, K. H., Zhang, Y., Duc, A. E., Rao, S., Hale, J. S., Academia, E. C., Shah, S. R., Morton, J. F., Holstein, C. A., Martin, D. B., Kaeberlein, M., Ladiges, W. C., Fink, P. J., MacKay, V. L., Weist, D. L. & Kennedy, B. K. The ribosomal protein RPL22

controls ribosome composition by directly repressing expression of its own paralog, RPL22L1. *PLoS Genetics* **9**, (2013).

13. Kurosawa, H. Methods for inducing embryoid body formation: In vitro differentiation system of embryonic stem cells. *Journal of Bioscience and Bioengineering* **103**, 389–398 (2007).

14. Zeevaert, K., Elsafi Mabrouk, M. H., Wagner, W. & Goetzke, R. Cell Mechanics in embryoid bodies. *Cells* **9**, 2270 (2020).

15. Dixon, J. E., Shah, D. A., Rogers, C., Hall, S., Weston, N., Parmenter, C. D., McNally, D., Denning, C. & Shakesheff, K. M. Combined hydrogels that switch human pluripotent stem cells from self-renewal to differentiation. Proceedings of the National Academy of Sciences 111, 5580–5585 (2014).

16. Fahl, S. P., Wang, M., Zhang, Y., Duc, A.-C. E. & Wiest, D. L. Regulatory roles of rpl22 in hematopoiesis: An old dog with new tricks. *Critical Reviews in Immunology* **35**, 379–400 (2015).

17. Fahl, S. P. Sertori, R., Zhang, Y., Contreras, A. V., Harris, B., Wang, M., Perrigoue, J., Balachandran, S., Kennedy, B. K. & Wiest, D. L. Loss of ribosomal protein paralog RPL22-like1 blocks lymphoid development without affecting protein synthesis. *The Journal of Immunology* **208**, 870–880 (2022).

18. MacCord, K. Germ Layers. *The Embryo Project Encyclopedia* (2013). Available at: https://embryo.asu.edu/pages/germ-layers. (Accessed: 15th August 2022)

19. MacCord, K. Endoderm. *The Embryo Project Encyclopedia* (2013). Available at: https://embryo.asu.edu/pages/endoderm. (Accessed: 15th August 2022)

20. MacCord, K. Mesoderm. *The Embryo Project Encyclopedia* (2013). Available at: https://embryo.asu.edu/pages/mesoderm. (Accessed: 15th August 2022)

21. MacCord, K. Ectoderm. *The Embryo Project Encyclopedia* (2013). Available at: https://embryo.asu.edu/pages/ectoderm. (Accessed: 15th August 2022)

22. Ogaki, S., Omori, H., Morooka, M., Shiraki, N., Ishida, S. & Kume, S. Late stage definitive endodermal differentiation can be defined by DAF1 expression. *BMC Developmental Biology* **16**, (2016).

23. D'Amour, K. A., Agulnick, A. D., Eliazer, S., Kelly, O. G., Kroon, E. & Baetge, E. E. Efficient differentiation of human embryonic stem cells to definitive endoderm. *Nature Biotechnology* **23**, 1534–1541 (2005).

24. Ma, Q., Jones, D., Borghesani, P. R., Segal, R. A., Nagasawa, T., Kishimoto, T., Bronson, R. T. & Springer, T. A. Impaired B-lymphopoiesis, myelopoiesis, and derailed cerebellar neuron migration in CXCR4- and SDF-1-deficient mice. *Proceedings of the National Academy of Sciences* **95**, 9448–9453 (1998).

25. Jiang, W., Zhang, D., Bursac, N. & Zhang, Y. WNT3 is a biomarker capable of predicting the definitive endoderm differentiation potential of hescs. *Stem Cell Reports* **1**, 46–52 (2013).

26. Wilkinson, D. G., Bhatt, S. & Herrmann, B. G. Expression pattern of the mouse T gene and its role in Mesoderm Formation. *Nature* **343**, 657–659 (1990).

27. Evseenko, D., Zhu, Y., Schenke-Layland, K., Kuo, J., Latour, B., Ge, S., Scholes, J., Dravid, G., Li, X., MacLellan, W. R. & Crooks, G. M. Mapping the first stages of mesoderm commitment during differentiation of human embryonic stem cells. *Proceedings of the National Academy of Sciences* **107**, 13742–13747 (2010).

28. Yang, L., Soonpaa, M. H., Adler, E. D., Roepke, T. K., Kattman, S. J., Kennedy, M., Henckaerts, E., Bonham, K., Abbott, G. W., Linden, R. M., Field, L. J. & Keller G. M. Human cardiovascular progenitor cells develop from a KDR+ embryonic-stem-cell-derived population. *Nature* **453**, 524–528 (2008).

29. Wang, Q., Zou, Y., Nowotschin, S., Kim, S. Y., Li, Q. V., Soh, C., Su, J., Zhang, C., Shu, W., Xi, Q., Huangfu, D., Hadjantonakis, A. & Massagué, J.The p53 family coordinates Wnt and nodal inputs in mesendodermal differentiation of embryonic stem cells. *Cell Stem Cell* **20**, 70–86 (2017).

30. Cao, B., Fang, Z., Liao, P., Zhou, X., Xiong, J., Zeng, S. & Lu H. Cancer-mutated ribosome protein L22 (RPL22/EL22) suppresses cancer cell survival by blocking p53-MDM2 circuit. *Oncotarget* **8**, 90651–90661 (2017).

31. Li, R., Bernau, K., Sandbo, N., Gu, J., Preissl, S. & Sun, X. PDGFRA marks a cellular lineage with distinct contributions to myofibroblasts in lung maturation and injury response. *eLife* **7**, (2018).

32. Goldman, D. C., Bailey, A. S., Pfaffle, D. L., Al Masri, A., Christian, J. L. & Fleming W. H. BMP4 regulates the hematopoietic stem cell niche. *Blood* **114**, 4393–4401 (2009).

33. Pevny, L. H., Sockanathan, S., Placzek, M. & Lovell-Badge, R. A role for Sox1 in neural determination. *Development* **125**, 1967–1978 (1998).

34. Suzuki, S., Namiki, J., Shibata, S., Mastuzaki, Y. & Okano, H. The neural stem/progenitor cell marker NESTIN is expressed in proliferative endothelial cells, but not in mature vasculature. *Journal of Histochemistry & Cytochemistry* **58**, 721–730 (2010).

35. Feng, L., Hatten, M. E. & Heintz, N. Brain lipid-binding protein (BLBP): A novel signaling system in the developing mammalian CNS. *Neuron* **12**, 895–908 (1994).

36. Gagliardi, D., Pagliari, E., Meneri, M., Melzi, V., Rizzo, F., Comi, G. P., Corti, S., Taiana, M. & Nizzardo, M. Stathmins and motor neuron diseases: Pathophysiology and therapeutic targets. *Biomedicines* **10**, 711 (2022).

37. Pataskar, A., Jung, J., Smialowski, P., Noack, F., Calegari, F., Staub, T. & Tiwari, V. K. Neurod1 reprograms chromatin and transcription factor landscapes to induce the neuronal program. *The EMBO Journal* **35**, 24–45 (2015).